

Aus dem Institut für Zahn-, Mund- und Kieferheilkunde  
der Medizinischen Fakultät Charité – Universitätsmedizin Berlin

**DISSERTATION**

**Auswertung von Prozessparametern zur Herstellung winziger  
biomedizinischer Geräte mittels 3D-Druck von PEEK**

**Evaluation of process parameters for the manufacture of tiny biomedical  
devices via 3D printing of PEEK**

zur Erlangung des akademischen Grades  
Doctor medicinae dentariae (Dr. med. dent.)

vorgelegt der Medizinischen Fakultät  
Charité – Universitätsmedizin Berlin

von  
Yiqiao Wang  
aus Hebei, China

Datum der Promotion: 17.09.2021

## Table of Contents

<b>List of Abbreviations</b> .....	1
<b>Abstract (English)</b> .....	2
<b>Abstract (Deutsch)</b> .....	3
<b>Synopsis</b> .....	4
1. Introduction / Objectives .....	4
2. Material and Methods.....	8
2.1 Materials and printer.....	8
2.2 Printing procedure and sample design.....	8
2.2.1 Optimal solutions for pure PEEK printing .....	8
2.2.2 Dental implants.....	9
2.3 Analysis methods.....	10
3. Results .....	12
3.1 RSM experiment.....	12
3.1.1 Density and dimension accuracy .....	12
3.1.2 Bending and compression tests.....	16
3.2 Implant design experiment.....	24
3.3 Implant printing .....	26
3.3.1 Implant printed with Apium HPP155 printer .....	26
3.3.2 Implants printed with Orion printer.....	27
4. Discussion .....	29
5. Conclusions and clinical implications .....	34
6. Reference.....	35
<b>Statutory Declaration</b> .....	39
<b>Declaration of Your Own Contribution to the Publications</b> .....	40
<b>Extract from the Journal Summary List</b> .....	41
<b>Printed Copy of the Publication</b> .....	46
<b>Curriculum Vitae</b> .....	62
<b>Publication List</b> .....	63
<b>Acknowledgment</b> .....	64

## List of Abbreviations

<b>PAEKs</b>	Poly-aryl-ether-ketone family
<b>PEEK</b>	Polyether ether ketone
<b>PEK</b>	Polyether ketone
<b>PEEKK</b>	Polyether ether ketoneketone
<b>ePEEK</b>	Epoxy-functionalized PEEK
<b>e/k</b>	Ratio of the ether bond to the ketone base
<b>AM</b>	Additive manufacturing
<b>FFF</b>	Fused filament fabrication
<b>SLS</b>	Selective laser sintering
<b>RSM</b>	Response surface method
<b>DOE</b>	Design-of-experiment
<b>T<sub>g</sub></b>	Glass transition temperature
<b>T<sub>m</sub></b>	Melting temperature
<b>σ<sub>B</sub></b>	Bending strength
<b>E<sub>B</sub></b>	Bending modulus
<b>F<sub>0.2%</sub></b>	Compression strength at 0.2 % plastic deformation
<b>E<sub>mod</sub></b>	Elastic modulus
<b>FEA</b>	Finite element analysis
<b>ANOVA</b>	Analysis of variance

## **Abstract**

**Objectives:** The experiments were designed to optimize the combinations of 3D-printing parameters for PEEK with a fused filament fabrication (FFF) process and to quantitatively evaluate the quality of 3D printed small parts, with the ultimate objective to 3D print small PEEK parts such as personalized dental implants.

**Methods:** This research was conducted using an experimental FFF 3D printer and PEEK filament. Standard PEEK parts were 3D printed for bending and compression tests. Based on the Box-Behnken design, a three factors based experiment was designed using Response Surface Methodology (RSM). Nozzle diameter, nozzle temperature and printing speed were involved. The density and dimensional accuracy of these printed parts were evaluated, and the bending and compression tests were conducted. With the optimized parameters, dental implants were printed with the same printing system.

**Results:** The nozzle diameter was found to be the most significant parameter affecting the bending and compression performance of the printed PEEK samples, followed by printing speed and nozzle temperature. The highest accuracy in sample width was obtained with a 0.6 mm nozzle while the most accurate diameter was obtained with a 0.4 mm nozzle. A combination of 0.4 mm nozzle diameter, 430 °C nozzle temperature and printing speed of 5 mm/s was beneficial to get the densest samples and therefore the best bending strength; reduced internal defects were possible with a 0.2 mm nozzle, a higher nozzle temperature of 440 °C and slower printing speed thus performed better bending modulus. The best compression properties were achieved with 0.6mm nozzles, with relatively low influence of the other parameters. Dental implants printed with 0.15 mm nozzle were achieved in our experiment.

**Conclusions:** Optimal parameter combinations have been found to get the best bending or compression properties. The optimized parameters for better dimension accuracy were also obtained depending on the shape of the specimens. Dental implants made from PEEK were printed for the first time.

## Zusammenfassung

**Ziel:** Die Experimente wurden entwickelt, um die Kombinationen von 3D-Druckparametern für PEEK mit einem FFF-Verfahren (Fused Filament Fabrication) zu optimieren und die Qualität von 3D-gedruckten Kleinteilen quantitativ zu bewerten, mit dem Ziel, kleine PEEK-Teile wie zum Beispiel personalisierte dentale Implantate in 3D zu drucken.

**Methoden:** Diese Forschung wurde unter Verwendung eines experimentellen FFF-3D-Druckers und eines PEEK-Filaments durchgeführt. Standard-PEEK-Teile wurden für Biege- und Drucktests in 3D gedruckt. Basierend auf dem Box-Behnken-Design wurde ein auf drei Faktoren basierendes Experiment unter Verwendung der Response Surface Methodology (RSM) entworfen. Düsendurchmesser, Düsentemperatur und Druckgeschwindigkeit waren beteiligt. Die Dichte und Maßgenauigkeit dieser gedruckten Teile wurden bewertet und die Biege- und Kompressionstests wurden durchgeführt. Mit den optimierten Parametern wurden Zahnimplantate mit demselben Drucksystem gedruckt.

**Ergebnisse:** Es wurde festgestellt, dass der Düsendurchmesser der wichtigste Parameter ist, der die Biege- und Kompressionsleistung der gedruckten PEEK-Proben beeinflusst, gefolgt von der Druckgeschwindigkeit und der Düsentemperatur. Die höchste Genauigkeit der Probenbreite wurde mit einer 0,6 mm-Düse erzielt, während der genaueste Durchmesser mit einer 0,4 mm-Düse erzielt wurde. Eine Kombination aus 0,4 mm Düsendurchmesser, 430 °C Düsentemperatur und Druckgeschwindigkeit von 5 mm / s war vorteilhaft, um die dichtesten Proben und damit die beste Biegefestigkeit zu erhalten; Reduzierte innere Defekte waren mit einer 0,2 mm-Düse, einer höheren Düsentemperatur von 440 °C und einer langsameren Druckgeschwindigkeit möglich, wodurch ein besserer Biegemodul erzielt wurde. Die besten Kompressionseigenschaften wurden mit 0,6-mm-Düsen bei relativ geringem Einfluss der anderen Parameter erzielt. In unserem Experiment wurden Zahnimplantate mit einer 0,15 mm Düse erhalten.

**Schlussfolgerungen:** Es wurden optimale Parameterkombinationen gefunden, um die besten Biege- oder Kompressionseigenschaften zu erzielen. Die optimierten Parameter für eine bessere Maßgenauigkeit wurden auch in Abhängigkeit von der Form der Proben erhalten. Zum ersten Mal wurden Zahnimplantate aus PEEK gedruckt.

## Synopsis

Evaluation of process parameters for the manufacture of tiny biomedical devices via 3D printing of PEEK

### 1. Introduction / Objectives

During the last decade, implantology has become an indispensable part of mainstream dentistry, helping dentists to improve the life quality of large patient populations. The dental implants often take the form of a screw that is composed of titanium, titanium alloy or ceramic, which is widely accepted by most implant manufacturers. But the elastic modulus of titanium are 110 GPa, which is almost 8 times greater than that of compact bone [1], and case reports as well as clinical studies showed that some patients are metal allergic after exposure to titanium [2,3]. Alternative implants made of zirconia have been launched which are almost twice as stiff as titanium implants (elastic modulus: 210 GPa) and there is still no evidence about their long-term success [4]. The high elastic modulus of these materials may cause the stress-shielding phenomenon, therefore, leading to marginal bone loss on functional loading at the surgical site [5]. Therefore polyether ether ketone (PEEK) dental implants seem to be promising substitutes concerning these disadvantages of traditional ones. Being considered as the leading thermoplastic candidate for replacing metal implant components, PEEK parts such as spine cages and retaining ring for acetabula cup assembly have especially potential in orthopedics [6–8] and trauma [9] due to its cortical bone-like elastic modulus.

PEEK is one of the most important members of the Poly-aryl-ether-ketone (PAEKs), which is a family of high-performance thermoplastic polymers, consisting of an aromatic backbone molecular chain, interconnected by ketone and ether functional groups [10]. With a melting point ( $T_m$ ) of 334 °C and glass transition temperature ( $T_g$ ) of 143 °C, PEEK is resistant to high temperatures and chemical corrosion. PEEK also possesses superior mechanical properties in strength, elastic modulus and fracture toughness when compared to other thermoplastics [11].

Many techniques are used to produce implantable devices of PEEK for medical applications. Traditional manufacturing process methods include injection moulding, extrusion, compression moulding, machining and so on [12]. Additionally, advancements in additive manufacturing are providing new opportunities for biomedical applications by enabling the creation of more complex architectures e.g. for tissue engineering scaffolding and patient personalized implants. SLS technique was used a decade ago in the PEEK 3D printing, which is a type of powder-based

AM technology. It is capable of fabricating porous PEEK-based composites with very complex architectures, permitting greater freedom of design [13]. Both 3D Systems and EOS have commercialized PEEK in their SLS machines. However, the high cost and concentrated laser beam restrict it from sintering large areas or laminates. In 2019, Lee et al. [14] reported their efforts towards 3D printing of PEEK by direct-ink writing technology at room temperature, which was enabled by a unique formulation comprised of commercial PEEK powder, soluble epoxy-functionalized PEEK (ePEEK), and fenchone. This combination formed a Bingham plastic that could be extruded using a readily available direct-ink write printer.

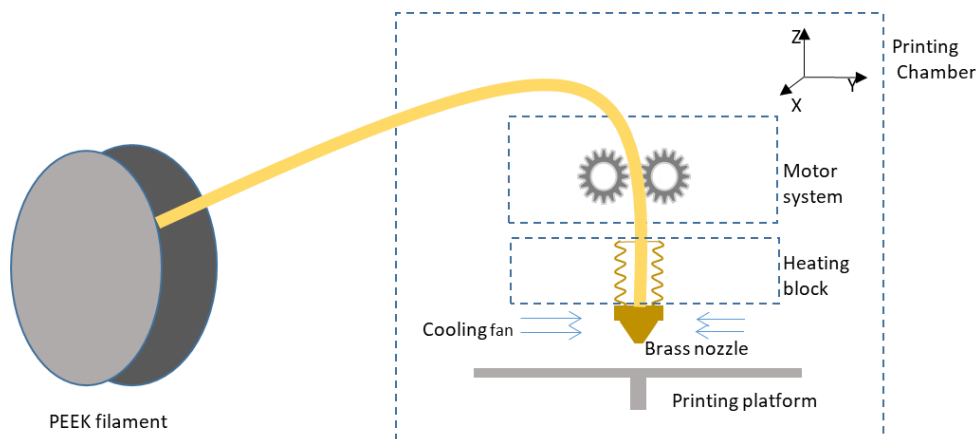


**Figure 1.** Schematic diagram of FFF 3D PEEK printer [15].

Besides the techniques mentioned above, fused filament fabrication (FFF) is currently the most widely used 3D printing strategy and a low-cost technology for thermoplastic materials [16]. In the FFF process, a filament is extruded from a nozzle continuously while heated to semiliquid state, then the filament rapidly adheres with the surrounding material and solidifies, and deposit follow a certain routine to form a desired shape [17], the schematic of FFF PEEK printer is showed in Figure 1. Many scholars reported their efforts in printing PEEK parts with FFF method. Wu et al. [18] investigated layer thickness and raster angle and found that the optimal mechanical properties of PEEK parts were achieved in samples with 0.3 mm layer thickness formed with a raster angle of 0°/90°. Deng et al. [19] conducted orthogonal array tests of four factors and three levels to investigate the effects of printing speed, layer thickness, printing temperature, and filling ratio on the tensile properties. Optimal tensile properties of the PEEK specimens were observed at a printing speed of 60 mm/s, the layer thickness of 0.2 mm, the temperature of 370 °C, and filling ratio of 40%. A study by Geng et al. [20] demonstrated the effects of the extrusion speed and printing speed on the microstructure and dimensions of an

extruded PEEK filament in 3D printing. They concluded that higher melt pressure is beneficial to reducing surface defects of the extruded filament. The work of Hu et al. [21] suggests a design for the improvement of FFF printing of PEEK where the nozzle is augmented by a heat collector which attempts to increase the temperature field of the printed material around the nozzle which resulted in an increase in overall strength. This design also incorporated a two-degree-of-freedom platform to reduce the warping of the build plate caused by the high ambient temperature. The articles conducting mechanical tests of 3D printed PEEK show that temperature, raster angle, layer thickness, filling ratio and printing speed are the main factors influencing the mechanical properties of printed PEEK. The optimal tensile, bending and compression properties of 3D printed pure PEEK specimens of the former researches are summarized in Table 1.

However, despite the many articles discussing FFF printing of PEEK, no consensus was reached on the optimal parameters for PEEK printing and the best mechanical properties have yet to be achieved. To date, there have been many applications of printed PEEK parts in the medical field such as spine cages, substitutes for maxillofacial or cranial bones and chest bones, however, no efforts have been made to adapt this technique to a smaller scale to print devices such as dental implants. Therefore, based on the experiences in former research, the aim of the present study was to develop an FFF process with optimal 3D printing parameters to print standard PEEK samples, the influences of printing parameters and their combinations on the appearance of finished parts were systematically studied through statistical design-of-experiment (DOE), with the ultimate objective to 3D print small PEEK parts such as personalized dental implants.



**Table 1.** The optimal results of literature and correspondent parameters [15].

Author	Most Significant Parameters	Tensile test		Bending test		Compression test	
		Tensile strength	Tensile modulus	Bending strength	Bending modulus	Compressive strength	Elastic modulus
		(Mpa)	(Gpa)	(Mpa)	(Gpa)	(Mpa)	(Gpa)
Wu et al. [18]	Layer thickness=300µm; raster angel=0/90°	56.60		56.10		60.90	
Vaezi et al. [22]	100% infill rate PEEK	75.06					
	/			132.37	2.43	102.38	
Rahman et al. [23]	Infill=100%; layer height=0.25 mm; nozzle temperature=340 °C; platform temperature=230 °C; printing speed=50 mm/s; raster angel=0 °	73.00	2.6-2.8	111.70	1.8-1.9	80.90	2.00
Yang et al. [17]	Nozzle temperature=420°C	59.00	3.10				
	Cooling method- annealing	81.50	3.90				
	Ambient temperature=150°C	85.00	3.90				
Berretta et al. [24]	PEEK 450G (380°C)	90.00					
	1% CNT PEEK 450G (365°C)	90.00					
	5% CNT PEEK 450G (350°C)	94.00					
Cicala et al. [25]	/	69.04 ±7.01	3.53 ±0.01				
Deng et al. [19]	Printing speed= 60 mm/s; layer thickness= 0.25 mm; printing temperature=370 °C; filling rate=60%	40±4.4	0.50				
Han et al. [26]	PEEK	95.21 ±1.86	3.79 ±0.27	140.83 ±1.97	3.56 ±0.13	138.63 ±2.69	2.79 ±0.11
	CFR-PEEK	101.41 ±4.23	7.37 ±1.22	159.25 ±13.54	5.41 ±0.51	137.11 ±3.43	3.51 ±2.12
Li et al. [27]	PEEK			146 ±3.3	3.44 ±0.05		
	CF-PEEK			146 ±4.2	3.74 ±0.09		
Hu et al. [21]	PEEK	74.70	1.15	120.20	1.15		
Reference	VICTREX® PEEK 450G moulded PEEK	98.00	4.00	165.00	3.80	125.00	3.80

## **2. Material and Methods**

### **2.1 Materials and printer**

The PEEK filament used in the experiment was VESTAKEEP<sup>®</sup> (Evonik, Germany) with a diameter of 1.75mm. The filament was dried in an oven at a temperature of 105 °C for 10 hours before printing and was stored in a closed box with desiccant during the experiment. A commercially available FDM printer (Orion AM GmbH, Berlin, Germany) designed for industrial additive manufacturing was used as the experimental system in our research. We created stl. files with Solidworks 2018 (Dassault Systemes, Waltham, MA) and accomplished the setting of printing parameters with the software Simplify 3D Version 4.1.1 (Simplify3D, US).

### **2.2 Printing procedure and sample design**

#### **2.2.1 Optimal solutions for pure PEEK printing**

In order to reveal the ideal parameter combinations for PEEK 3D printing with respect to the mechanical properties, Response Surface Methodology (RSM) was used by creating a Box-Behnken design based on three parameters with three levels, namely nozzle diameter (0.2, 0.4 and 0.6 mm), nozzle temperature (420, 430 and 440 °C) and printing speed (5, 10 and 15 mm/s), resulting in 27 groups, whereas due to the Box-Behnken design, 13 different parameter combinations, with one combination repeated 5 times, were necessary to evaluate (Table 2). Based on these combinations of the printing parameters, specimens were 3D printed for three-point bending tests (B) and compression tests (C), resulting in 2 x 17 groups (B1- B17 and C1- C17) consisting of n=5 specimens per test specification. The three-point bending tests specimens in the shape of small bars (length: 18 mm, width: 6 mm, height: 2 mm) and the compression tests cylindrical specimens (height: 10 mm, diameter: 5 mm) were printed from PEEK according to the ISO standard 178 and ISO standard 604, respectively. The printing direction is shown in Figure 2, other parameters such as layer thickness (0.1 mm), plate temperature (250 °C) and infill ratio/ pattern (100 % rectilinear) were not changed. All of the samples were printed in a closed chamber and cooled down to room temperature naturally.

**Table 2.** Overview of the different groups due to different combinations of the three parameters.

Groups	Nozzle diameter (mm)			Nozzle temperature ( °C)			Printing speed (mm/s)		
	x	y	z	x	y	z	x	y	z
1	0.6	440	10						
2	0.6	430	15						
3	0.6	430	5						
4	0.6	420	10						
5	0.4	440	15						
6	0.4	440	5						
7	0.4	430	10						
8	0.4	430	10						
9	0.4	430	10						
10	0.4	430	10						
11	0.4	430	10						
12	0.4	420	15						
13	0.4	420	5						
14	0.2	440	10						
15	0.2	430	15						
16	0.2	430	5						
17	0.2	420	10						

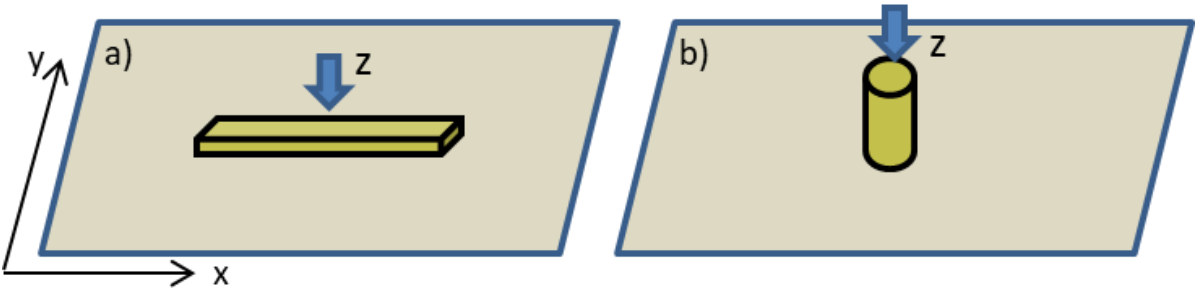


**Figure 2.** Schematic diagram of printing direction with the arrow representing the nozzle (a bending test samples, b compression test samples).

**2.2.2 Dental implants**

To pursue the possible design of dental implants by FDM, we also designed special shapes to explore the acceptable design. Starting from the cylindrical test specimen, further more complex

specimens were designed, whose shape gradually approximated that of dental implants with an external and internal thread (Figure 3). Printing conditions were kept same for all the cohorts (Table 3), and the printing direction was vertical to the longest edge of the samples. Model “e” was tried to print with a commercially available 3D printer for PEEK from Apium (Karlsruhe, Germany) as well as a printer from Orion (Berlin, Germany).

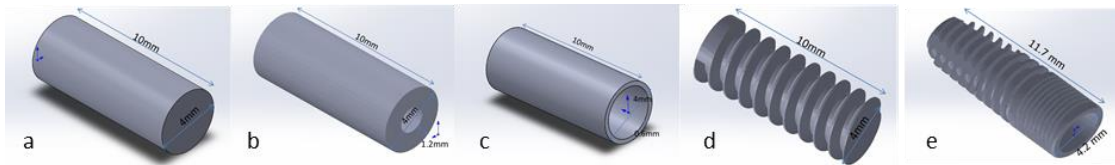


**Figure 3.** Specimens design of experiment (a is the concrete cylinder, b and c is the hollow cylinder with wall thickness of 1.2mm or 0.6mm, c is the cylinder with screw of metric die M10\*1.0 on the surface, d is dental implant, e is dental implant).

**Table 3.** Printing settings for FFF implants.

<b>Extruder</b>		<b>Infill</b>	
Nozzle diameter (mm)	0.15	Internal fill pattern	Rectilinear
Extrusion multiplier	0.98	External fill pattern	Rectilinear
Retraction distance (mm)	5	Interior fill percentage (%)	100
Retraction speed (mm/min)	1800		
Nozzle temperature (°C)	440	<b>Additions (skirt/brim)</b>	
		Skirt layers	3
<b>Layer</b>		Skirt offset from part (mm)	1
1st layer height (mm)	0.1	Skirt outlines	2
Top solid layers	3		
Bottom solid layer	3	<b>Other</b>	
Outline shells	3	Filament diameter (mm)	1.75
1st layer height (mm)	0.2	Cooling fan (%)	80
Bed temperature (°C)	250	Printing speed (mm/s)	5

### 2.3 Analysis methods

The microstructure of the printed devices was analyzed using an optical microscope VHX-5000F (Keyence, Osaka, Japan). The density of the samples was measured by an Archimedes density measuring instrument (KERN YDB-03, KERN & SOHN GmbH, Balingen, Germany) and compared with the density of PEEK in general ( $1.32 \text{ g/cm}^3$ ) [28]. The width of the bars and the

diameter of the cylinders were measured with a digital caliper and compared to the theoretical values of 6 mm and 5 mm, respectively. Three-point bending and compression tests were conducted using a universal testing machine (Z010, Zwick GmbH & Co, Ulm, Germany) with a constant crosshead speed of 1 mm/min and a preload of 1 N. The bars were strained with a test fin in the middle vertically to the wide edge of the sample and the cylinders were loaded with the test stamp along the long axis. Bending modulus, maximum bending strength, elastic modulus and the strength at 0.2 % plastic deformation during compression were recorded. Micro-computed tomography (micro-CT) scans were conducted with SKYSCAN 1275 (Bruker, Karlsruher, Germany) to detect the inner defects of printed implants.

For the purpose of revealing significant differences of the results, statistical analyses of variance (ANOVA) were performed using the software SPSS 25.0 (IBM SPSS Statistics, New York, USA). The level of significance was set at  $p < 0.05$ . The graphs were made using the software Origin 2018 (OriginLab, Northampton, Massachusetts, USA).

### 3. Results

#### 3.1 RSM experiment

##### 3.1.1 Density and dimension accuracy

In Figure 4 the microstructures of the sample surfaces are presented. The samples were chosen according to the parameter nozzle diameter. The samples printed with a 0.6 mm nozzle consisted of the widest contour, infill lines, and the highest contour/ infill line ratio, while the samples of the 0.2 mm nozzle groups had the least (Figure 4A, B and D). The images of surfaces along the z-axis showed more homogenous structures of the layers in the 0.6 mm nozzle groups, whereas the samples printed with a 0.4 mm and 0.2 mm nozzle showed dislocation and defects (Figure 4C and E).

The densities and dimensions of the bars and cylindrical samples are shown in Table 4. The highest densities were observed for B6 ( $1.274 \pm 0.003 \text{ g/cm}^3$ ) and C1 ( $1.278 \pm 0.003 \text{ g/cm}^3$ ) and the lowest densities were observed for B14 ( $1.165 \pm 0.009 \text{ g/cm}^3$ ) and C15 ( $1.185 \pm 0.010 \text{ g/cm}^3$ ). The density of these 100 % infilled printed PEEK parts ranged between 88.3 % and 96.5 % for the bars and between 89.8 % and 96.8 % for the cylinders compared to the density of PEEK in general. The least dimensional deviations was shown for B14 ( $0.006 \pm 0.019 \text{ mm}$ , 0.10 %) and C9 ( $0.077 \pm 0.005 \text{ mm}$ , 1.54 %) and the maximal dimensional deviations could be shown for B6 ( $0.245 \pm 0.090 \text{ mm}$ , 4.08 %) and C2 ( $0.214 \pm 0.024 \text{ mm}$ , 4.28 %).

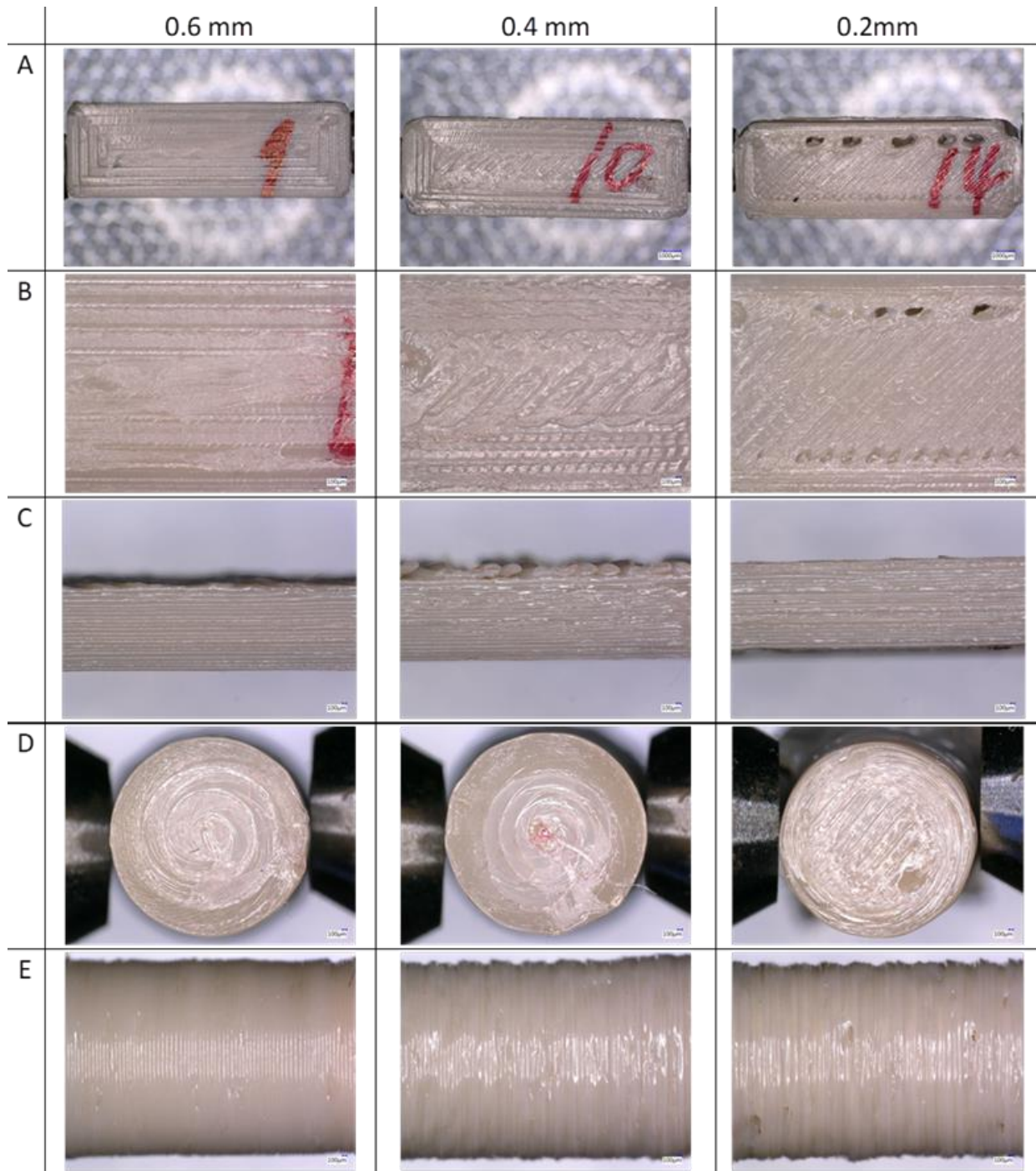


**Figure 4.** Microscope pictures of bending and compression samples with Keyence (A: x/y plane of bars, showing the deposition patterns, x20; B: close up picture of x/y plane, x50; C: close up of z-axis of bending samples, x50; D: close up of x/y plane of cylinders, x50; E: close up of z-axis of cylinders, x50)

**Table 4.** The measured density and dimensions of the bending (bars) and compression samples (cylinders)

Group number	Density (B-bending samples)	Density (C-compression samples)	Width (B-bending samples)	Deviation of the width of the bars (%)	Diameter (C-compression samples)	Deviation of the diameter of the cylinders (%)
	$\rho_B$ (g/cm <sup>3</sup> )	$\rho_C$ (g/cm <sup>3</sup> )	$\Phi_B$ (mm)	$\Phi_B'$	$\Phi_C$ (mm)	$\Phi_C'$
1	1.241 ± 0.004	1.278 ± 0.003	5.948 ± 0.012	0.87 ± 0.20	4.835 ± 0.022	3.30 ± 0.44
2	1.246 ± 0.009	1.268 ± 0.011	5.956 ± 0.014	0.73 ± 0.23	4.786 ± 0.024	4.28 ± 0.48
3	1.233 ± 0.003	1.276 ± 0.003	6.110 ± 0.028	1.83 ± 0.47	4.858 ± 0.029	2.84 ± 0.58
4	1.235 ± 0.003	1.272 ± 0.002	5.954 ± 0.020	0.77 ± 0.33	4.834 ± 0.015	3.32 ± 0.30
5	1.257 ± 0.002	1.242 ± 0.003	6.068 ± 0.017	1.13 ± 0.28	4.874 ± 0.017	2.52 ± 0.34
6	1.274 ± 0.003	1.271 ± 0.005	6.245 ± 0.090	4.08 ± 1.50	4.862 ± 0.013	2.76 ± 0.26
7	1.233 ± 0.015	1.218 ± 0.008	6.127 ± 0.017	2.12 ± 0.28	4.905 ± 0.012	1.90 ± 0.24
8	1.227 ± 0.002	1.224 ± 0.001	6.127 ± 0.021	2.12 ± 0.35	4.907 ± 0.009	1.86 ± 0.18
9	1.235 ± 0.005	1.229 ± 0.004	6.153 ± 0.019	2.55 ± 0.32	4.923 ± 0.005	1.54 ± 0.10
10	1.237 ± 0.002	1.220 ± 0.003	6.110 ± 0.014	1.83 ± 0.23	4.920 ± 0.008	1.60 ± 0.16
11	1.226 ± 0.019	1.220 ± 0.008	6.137 ± 0.031	2.28 ± 0.52	4.920 ± 0.016	1.60 ± 0.32
12	1.251 ± 0.007	1.240 ± 0.005	6.098 ± 0.025	1.63 ± 0.42	4.872 ± 0.023	2.56 ± 0.46
13	1.267 ± 0.003	1.241 ± 0.006	6.182 ± 0.040	3.03 ± 0.67	4.910 ± 0.018	1.80 ± 0.36
14	1.165 ± 0.009	1.233 ± 0.006	6.006 ± 0.019	0.10 ± 0.32	4.868 ± 0.022	2.64 ± 0.44
15	1.233 ± 0.007	1.185 ± 0.010	6.098 ± 0.029	1.63 ± 0.48	4.838 ± 0.026	3.24 ± 0.52
16	1.252 ± 0.009	1.195 ± 0.017	6.182 ± 0.079	3.03 ± 1.32	4.828 ± 0.007	3.44 ± 0.14
17	1.181 ± 0.020	1.187 ± 0.012	6.014 ± 0.022	0.23 ± 0.37	4.868 ± 0.012	2.64 ± 0.24

n=5



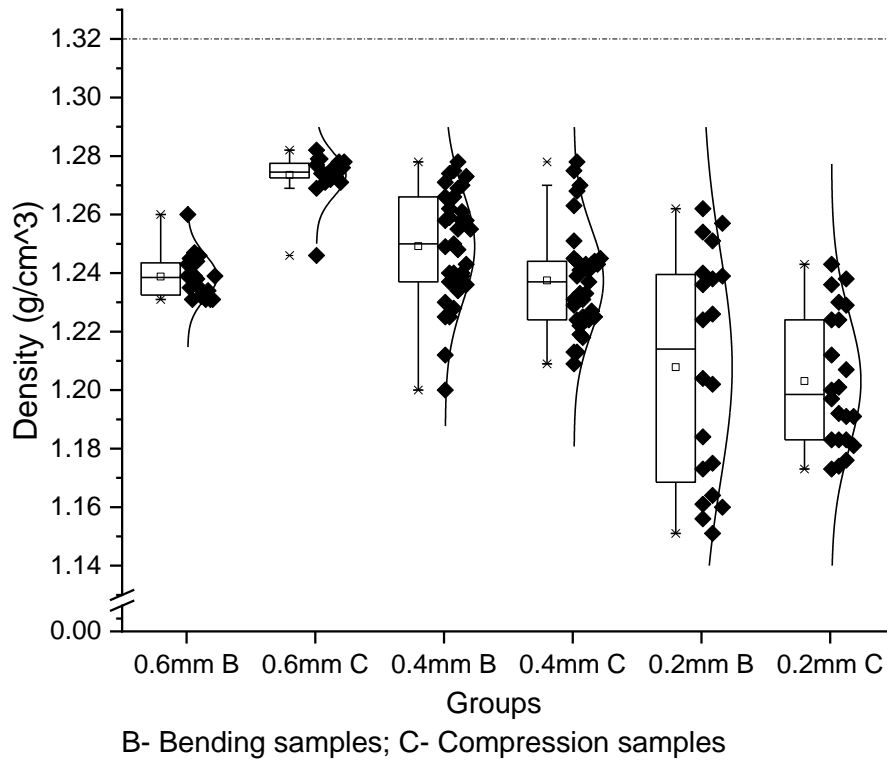


**Figure 5.** The densities of the PEEK bending bars and compression cylinders grouped according to the parameter nozzle diameter.

The bending samples printed with a 0.4 mm nozzle showed the highest density, while those printed with a 0.2 mm nozzle had the lowest density. The differences between the three groups were significant ( $p < 0.05$ ). The compression samples of the 0.6 mm groups were the most compact ones, followed by the 0.4 mm and the 0.2 mm groups. For both bar and cylinder samples, the values were most scattered in the 0.2 mm groups, indicating that printing speed and nozzle temperature had stronger influences on the density of samples printed with the 0.2 mm nozzles than on the ones printed with the 0.4 mm and 0.6 mm nozzles (Figure 5).

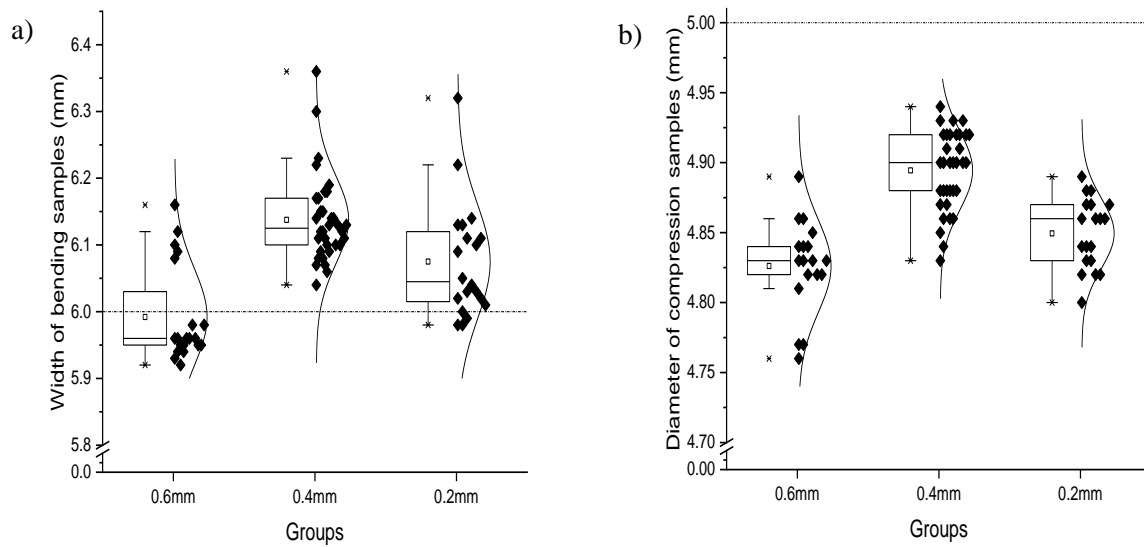


**Figure 6.** The dimensional accuracy of printed samples grouped according to the parameter nozzle diameter (a: widths of the PEEK bars; b: diameters of the PEEK cylinders).

Compared to the default width of bar samples of 6 mm, and the default diameter of cylindrical samples of 5 mm, all samples showed inaccuracy in dimension concerning the theoretical value (Figure 6). The bar width showed the least variance when applying the 0.6 mm nozzle of about 0.1 % on average, and the cylinder diameter showed the least shrinkage of about 2.1 % when applying a 0.4 mm nozzle. The differences between the three groups were significant ( $p < 0.05$ ).

### 3.1.2 Bending and compression tests

The design matrix and response (bending and compression performance index) are listed in Table 5. The highest bending strength combined with the lowest bending modulus was observed when using a 0.4 mm nozzle with a printing speed of 10 mm/s and nozzle temperature of 430°C (B8, B9). The use of a 0.6 mm nozzle resulted in the highest compression strengths between  $81.60 \pm 0.62$  MPa (C4) and  $87.00 \pm 1.02$  MPa (C1) in combination with the highest elastic modulus above 2 GPa.

**Table 5.** Summary of the results of the bending and compression tests.

Group number	Bending strength $\sigma_B$ (MPa)	Bending modulus $E_B$ (GPa)	Group number	Compression strength $F_{0.2\%}$ (MPa)	Elastic modulus $E_{mod}$ (GPa)
B1	73.26 ± 13.26	1.290 ± 0.035	C1	87.00 ± 1.02	2.098 ± 0.238
B2	64.70 ± 11.83	1.248 ± 0.052	C2	82.30 ± 3.58	2.104 ± 0.125
B3	127.20 ± 7.47	1.248 ± 0.087	C3	83.20 ± 2.70	2.008 ± 0.051
B4	51.40 ± 14.78	1.230 ± 0.046	C4	81.60 ± 0.62	2.193 ± 0.058
B5	163.75 ± 10.76	1.165 ± 0.105	C5	68.00 ± 4.04	1.733 ± 0.183
B6	184.40 ± 6.12	1.190 ± 0.127	C6	72.34 ± 5.81	1.550 ± 0.570
B7	181.33 ± 9.46	1.157 ± 0.046	C7	61.30 ± 1.84	1.663 ± 0.202
B8	193.33 ± 7.04	1.049 ± 0.097	C8	65.90 ± 1.63	1.593 ± 0.068
B9	185.33 ± 2.49	1.045 ± 0.048	C9	65.20 ± 1.02	1.633 ± 0.021
B10	188.00 ± 0.82	1.127 ± 0.038	C10	63.60 ± 2.05	1.633 ± 0.113
B11	186.00 ± 1.00	1.070 ± 0.010	C11	62.90 ± 4.30	1.635 ± 0.362
B12	156.60 ± 18.86	1.128 ± 0.075	C12	71.73 ± 3.99	1.663 ± 0.056
B13	184.40 ± 11.25	1.174 ± 0.101	C13	75.80 ± 3.49	1.857 ± 0.066
B14	141.40 ± 11.50	1.252 ± 0.089	C14	64.40 ± 3.66	1.730 ± 0.065
B15	151.00 ± 8.65	1.476 ± 0.103	C15	46.60 ± 3.42	1.456 ± 0.063
B16	155.40 ± 12.18	1.474 ± 0.106	C16	50.30 ± 3.90	1.494 ± 0.060
B17	114.60 ± 25.30	1.370 ± 0.039	C17	50.20 ± 2.30	1.602 ± 0.122

n=5

The stress-strain curves resulting from the bending and compression tests are shown in Figure 7 and the correspondent box-plot was shown in Figure 8. The results are grouped according to the parameter nozzle diameter.

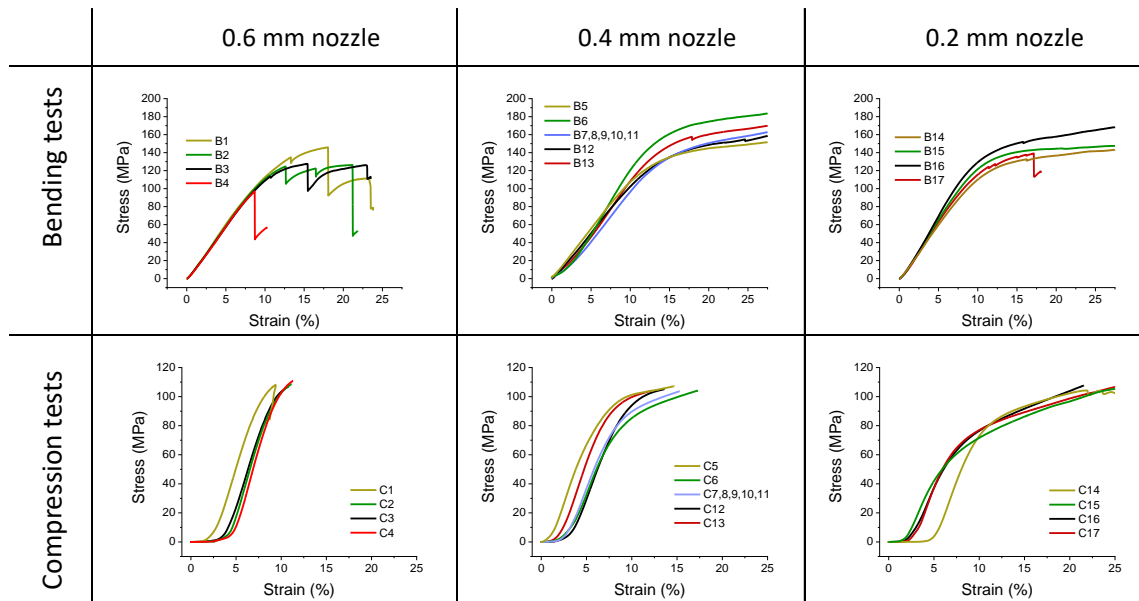


**Figure 7.** Representative stress-strain curves resulting from the three-point bending and compression tests of samples printed with different nozzle diameters.

The bending strengths of the samples showed a similar trend like the density, the maximal value was obtained with 0.4 mm nozzle for both. In the three-point bending test, all printed samples exhibited a linear elastic deformation at the beginning, and then reached a maximum of bending stress, whereas they did not break during the entire tests. The samples printed with a 0.6 mm nozzle were the stiffest, showing the least deformation, while the samples printed with a 0.2 mm nozzle were more flexible compared to the other samples, and the deformation of the force application position was the most visible. The curves of samples printed with 0.6 mm nozzle are more concentrated while the 0.2 mm and 0.4 mm groups' curves were more scattered (Figure 7).

The compression strength and modulus of the cylinders also showed the same trend as density. In the compression test, the compactness of samples printed with a 0.2 mm nozzle was the most obvious and showed the lowest compression strength and modulus, while the samples printed with a 0.6 mm nozzle showed the least deformations and performed the best in the static loading test. Therefore, the reduction of the cylinder heights due to the compression tests amounted to 0.93 %, 5.37 % and 9.58 % for the groups with a 0.6 mm, 0.4 mm and 0.2 mm nozzle diameter, respectively. All samples showed initial linear elastic behavior followed by plastic deformation. The plastic deformation of samples printed with 0.2 mm nozzle was the longest, while the 0.6 mm nozzle was the shortest (Figure 7).

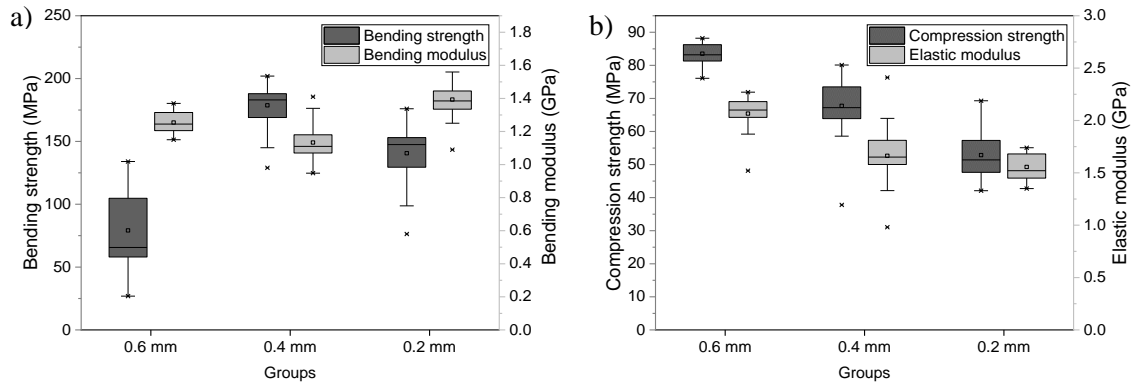


**Figure 8.** Results of the bending strengths and bending modulus (a) and the compression strengths and elastic modulus (b) based on different nozzle diameters.

The use of a 0.6 mm nozzle caused the lowest bending strength in the bending tests, whereas in the compression tests the highest compression strength was obtained with the same nozzle diameter. The highest bending modulus was achieved with a 0.2 mm nozzle in the bending tests, while this nozzle size caused the lowest elastic modulus in the compression tests (Figure 8). The differences between the three groups were significant ( $p < 0.05$ ).

For the following ANOVA of the regression model of the bending strength, bending modulus, compression strength and elastic modulus, the values  $R^2$ , adjusted  $R^2$ , predicted  $R^2$  and adequate precision (adeq. precision) are given. The results are summarized in Tables 6-9. An adjusted  $R^2 > 0.8$  indicates that the simulation of the equation was reliable. A predicted  $R^2$  in reasonable agreement with the adjusted  $R^2$  showing the difference less than 0.2 indicated the well predicts responses of the regression model for new observations. The adequate precision measures the signal to noise ratio. A ratio greater than 4 is desirable, indicating an adequate signal. Figures 9-12 show the surface response of the mechanical tests and the relationship index between predicted and actual (predicted vs. actual) values of results. The least significant parameter affecting the results of each mechanical property was taken as moderate value in the surface plot. The actual vs. predicted plot showed that all developed models were adequate because the residuals tend to be close to the diagonal line.

The regression equations of the established model are shown as follows (x- nozzle diameter, y- nozzle temperature, z- printing speed):

Bending strength  $\sigma_B = -40886.8625 + 1650.58*x + 189.44527*y - 18.40605*z - 0.6175*x*y - 14.525*x*z + 0.03575*y*z - 1741.81875*x^2 - 0.219602*y^2 + 0.29799*z^2$ . (1)

Bending modulus  $E_B = 6.80076 - 15.38079*x - 0.008963*y - 0.202557*z + 0.02225*x*y + 0.3515*x*z + 4.91349*x^2 + 0.010052*z^2 - 0.0176*x*z^2$  (2)

Compression strength  $F_{0.2\%} = -26.47029 + 76.625*x + 0.1555*y - 0.326*z$ . (3)

Elastic modulus  $E_{mod} = 190.61249 + 8.09474*x - 0.865788*y - 0.8229*z - 0.024125*x*y + 0.03375*x*z + 0.001885*y*z + 4.10658*x^2 + 0.000993*y^2$  (4)

### Bending strength

**Table 6.** ANOVA for quadratic model of bending strength ( $\sigma_B$ ).

Source	Sum of Squares	Mean Square	F-value	p-value
Model	33705.66	3745.07	70.82	< 0.0001
x-Nozzle diameter	7554.66	7554.66	142.85	< 0.0001
y-Nozzle temperature	389.34	389.34	7.36	0.0301
z-Printing speed	1663.2	1663.2	31.45	0.0008
Xy	6.1	6.1	0.1154	0.7441
Xz	843.9	843.9	15.96	0.0052
Yz	12.78	12.78	0.2417	0.638
x <sup>2</sup>	20439.12	20439.12	386.49	< 0.0001
y <sup>2</sup>	2030.54	2030.54	38.4	0.0004
z <sup>2</sup>	233.68	233.68	4.42	0.0736

$R^2=0.9891$ , adjusted  $R^2=0.9752$ , predicted  $R^2= 0.8587$ , adeq. precision=23.8821

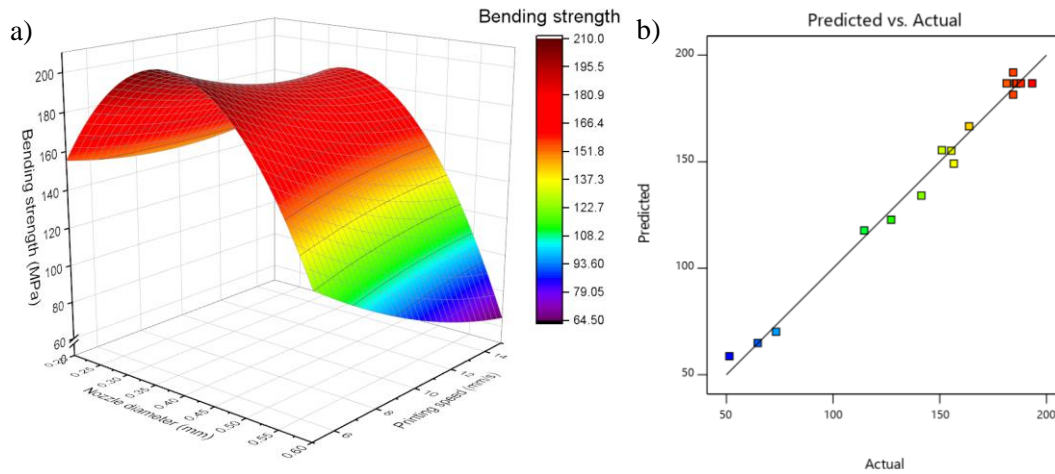


**Figure 9.** The analysis of the bending strengths (a: surface response for a nozzle temperature of 430°C; b: predicted and actual appearance index).

The coefficients of item x, y, z as well as the p-values showed the significance of parameters' influences. The ranking of parameters affecting bending strength was nozzle diameter (x) > printing speed (z) > nozzle temperature (y).

### Bending modulus

**Table 7.** ANOVA for reduced cubic model of bending modulus ( $E_B$ ).

Source	Sum of Squares	Mean Square	F-value	p-value
Model	0.2572	0.0322	20.94	0.0001
x-Nozzle diameter	0.0026	0.0026	1.69	0.2293
y-Nozzle temperature	3.13E-06	3.13E-06	0.002	0.9651
z-Printing speed	0.0006	0.0006	0.3877	0.5509
Xy	0.0079	0.0079	5.16	0.0528
Xz	1.00E-06	1.00E-06	0.0007	0.9803
x <sup>2</sup>	0.1631	0.1631	106.24	< 0.0001
z <sup>2</sup>	0.0239	0.0239	15.59	0.0042
xz <sup>2</sup>	0.0155	0.0155	10.09	0.0131

$R^2 = 0.9544$ , adjusted  $R^2 = 0.9089$ , predicted  $R^2 = 0.8212$ , adeq. precision = 13.8011

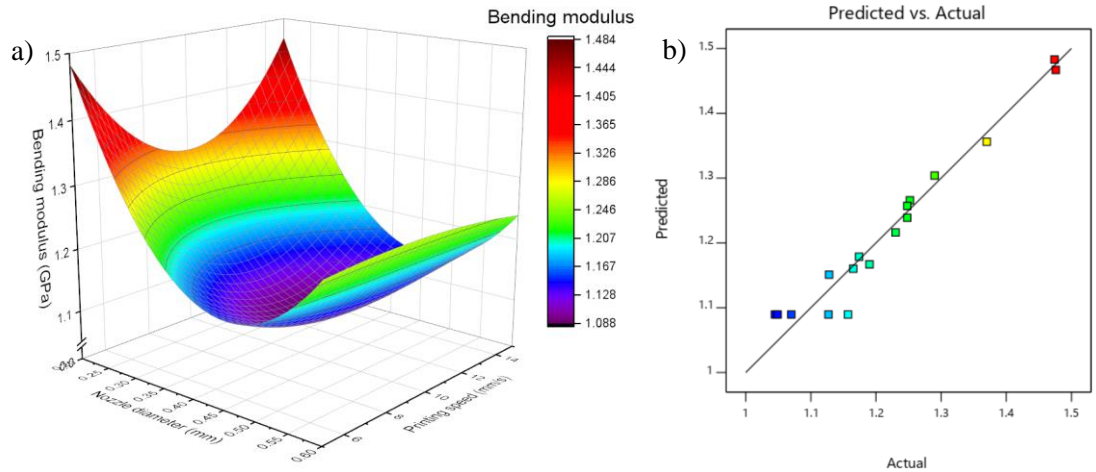


**Figure 10.** The analysis of the bending modulus (a: surface response for a nozzle temperature of 430°C; b: predicted and actual appearance index).

The nozzle diameter was related to the bending modulus, while the nozzle temperature hardly had effect on this performance. The significance ranking of parameters affecting bending modulus was nozzle diameter (x) > printing speed (z) > nozzle temperature (y).

### Compression strength

**Table 8.** ANOVA for linear model of compression strength ( $F_{0.2\%}$ ).

Source	Sum of Squares	Mean Square	F-value	p-value
Model	1919.44	639.81	23.22	< 0.0001
x-Nozzle diameter	1878.85	1878.85	68.19	< 0.0001
y-Nozzle temperature	19.34	19.34	0.7021	0.4172
z-Printing speed	21.26	21.26	0.7714	0.3957

$R^2 = 0.8427$ , adjusted  $R^2 = 0.8064$ , predicted  $R^2 = 0.7105$ , adeq. precision=13.3181



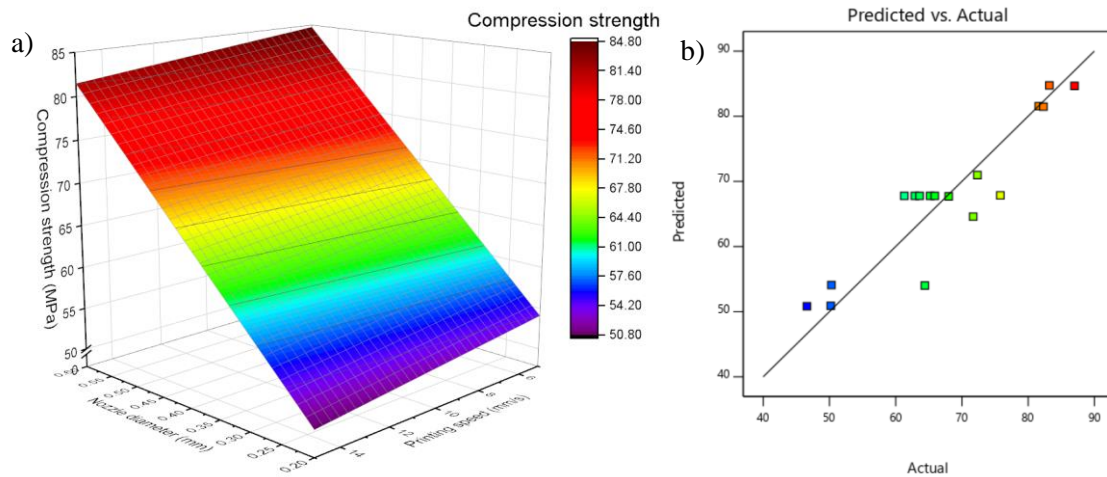


**Figure 11.** The analysis of the compression strengths (a: surface response for a nozzle temperature of 430°C; b: predicted and actual appearance index).

The influence of the three parameters was nozzle diameter (x) >> printing speed (z) > nozzle temperature (y). A bigger nozzle diameter and lower printing speed were more favorable to achieve higher compression strengths.

### Elastic modulus

**Table 9.** ANOVA for reduced quadratic model of elastic modulus ( $E_{mod}$ ).

Source	Sum of Squares	Mean Square	F-value	p-value
Model	0.798	0.0998	43.93	< 0.0001
x-Nozzle diameter	0.5778	0.5778	254.47	< 0.0001
y-Nozzle temperature	0.0068	0.0068	3.01	0.1207
z-Printing speed	0.0003	0.0003	0.1165	0.7417
xy	0.0093	0.0093	4.1	0.0774
xz	0.0046	0.0046	2.01	0.1944
yz	0.0355	0.0355	15.65	0.0042
x <sup>2</sup>	0.1139	0.1139	50.17	0.0001
y <sup>2</sup>	0.0416	0.0416	18.32	0.0027

$R^2=0.9777$ , adjusted  $R^2=0.9555$ , predicted  $R^2=0.8125$ , adeq. precision=21.4086

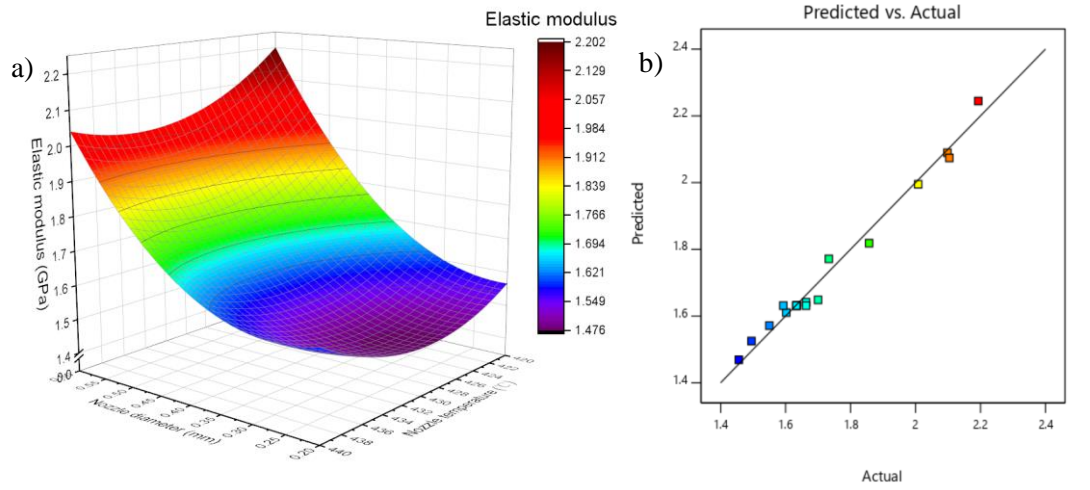


**Figure 12.** The analysis of the elastic modulus (a: surface response for a printing speed of 10mm/s; b: predicted and actual appearance index).

The influence of the three parameters was nozzle diameter (x) > nozzle temperature (y) > > printing speed (z).

### 3.2 Implant design experiment

To achieve the dimension accuracy of the sample, nozzle with a diameter of 0.15 mm was applied in this part. The other parameters were set as nozzle temperature of 440 °C, printing speed of 5 mm/s, lay height of 0.1 mm and plate temperature of 250 °C. The samples before and after compression test are shown in Figure 13. And the elastic modulus and the compression strength by 0.2 % deformation of the specimens are summarized in Table 10 and Figure 14.

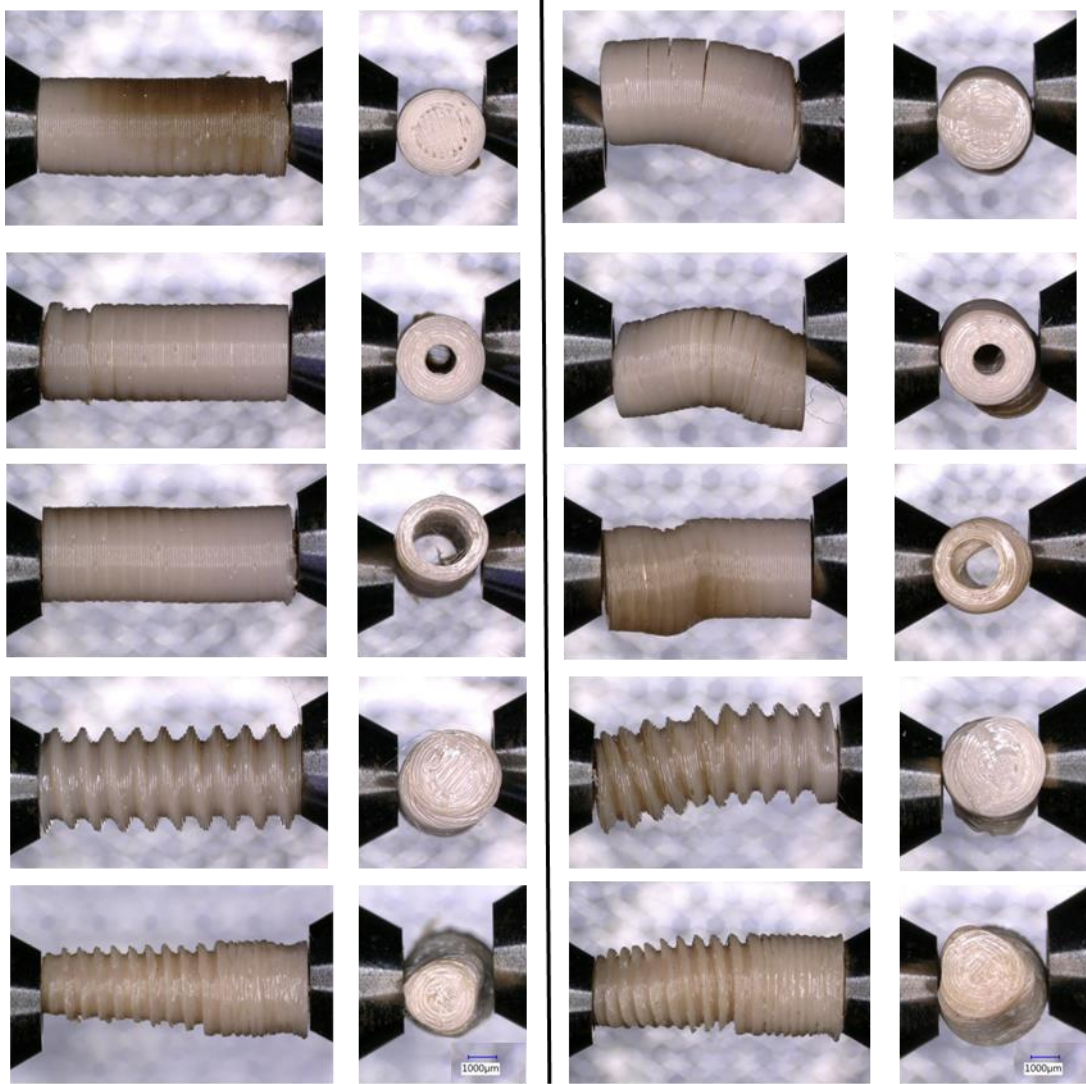


**Figure 13.** Comparison of samples before and after compression test.

**Table 10.** Compression strength of designed- shape samples.

	Concrete cylinder	Thick wall cylinder	Thin wall cylinder	Screwed cylinder	Implant
Compression strength (MPa)	$68.57 \pm 3.92$	$64.03 \pm 0.97$	$52.47 \pm 1.96$	$72.17 \pm 2.77$	$49.83 \pm 3.31$
Compression modulus(GPa)	$4.24 \pm 0.37$	$3.66 \pm 0.12$	$3.08 \pm 0.07$	$3.57 \pm 0.28$	$2.89 \pm 0.21$

n=5

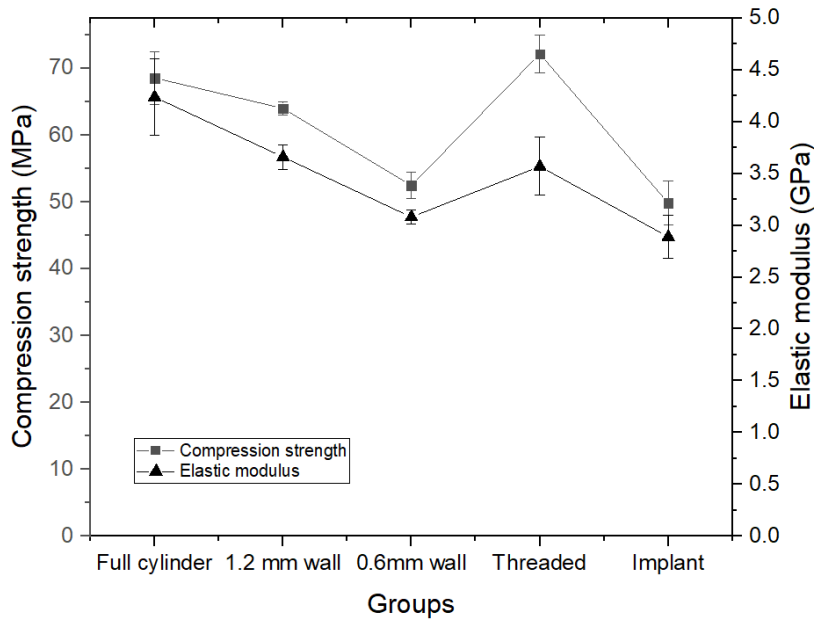


**Figure 14.** The compression strength and modulus of designed samples

From the results we can see that both decreasing the thickness of the wall and digging screws on the surface reduced the elastic modulus of the printed parts by 14 % to 28 %, compare with the full cylinder of the same specifications. The elastic modulus of the implants is  $2.89 \pm 0.21$  GPa, which matches well with the alveolar bone.

### 3.3 Implant printing

Based on the experiences from the literature survey and our own, it was tried to print a dental implant with an inner and outer structure using a commercial available 3D printer for PEEK from Apium (Karlsruhe, Germany) as well as a printer from Orion (Berlin, Germany).

#### 3.3.1 Implant printed with Apium HPP155 printer

We printed a magnified dental implant which is almost three times in dimension of a real one; applying the optimal parameters we got from others experience as well as our own trials, to explore the possibility to produce dental implant with FDM strategy. As we can see from the image (Figure 15), both the inner and outer screw depth of the implant is not acceptable and the porosity of sample is evident. Implants with smaller dimension were also tried but all of them are failed. Since there is not matching substitute nozzle with smaller nozzle diameter for this printer, we tried to print the implant with another printer from Orion, which is more flexible in nozzle and heater settings.

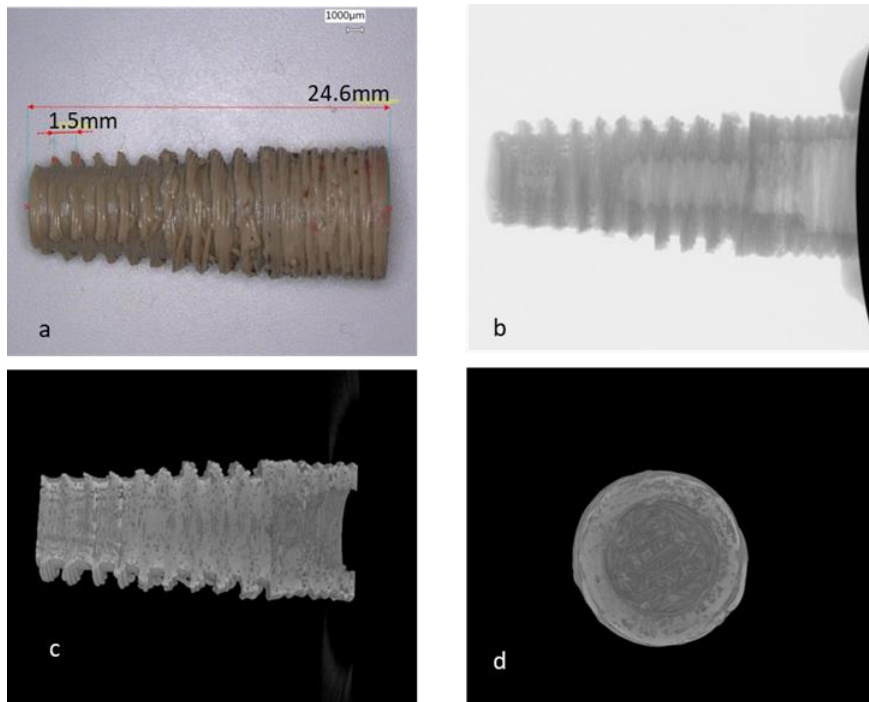


**Figure 15.** Images of a magnified dental implant produced with Apium HPP155 (a is the printed implant, b,c,d is micro CT of sample) [15].

### 3.3.2 Implants printed with Orion printer

We printed the same dental implant stl. file with the second generation printer of Orion, and get better results as showed in Figure 16. The smallest successfully printed implant is with the width of 3.6 mm and length of 9.4 mm, which is a little crooked. We get the best specimens with the 0.15 mm nozzle when printing the x1.2 scale implant, which is acceptable in both the reproducibility and surface quality, the parameters for printing are showed in Table 11. However, smaller nozzles will inevitably lead to long printing time and are more easily to be clogged. This may be ignorable at the research phase, but will increase the cost in manufacturing in mass.

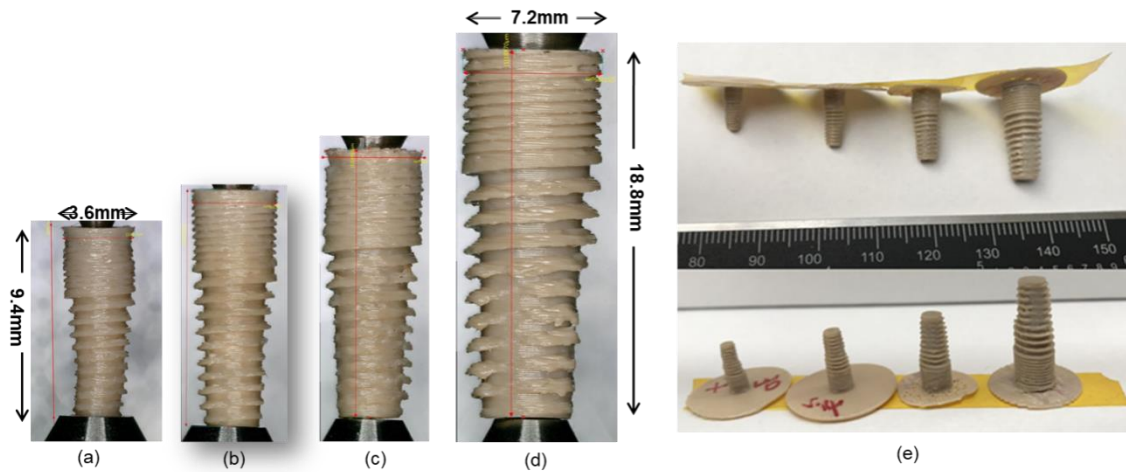


**Figure 16.** Dental Implants printed with Orion Generation 2 (b, c and d is x1.2, x1.5 and x2 scale of a separately; a and b is printed with 0.15mm nozzle at the temperature of 405°C, c is printed with 0.2mm nozzle at the temperature of 390°C, d is printed with 0.4mm nozzle at the temperature of 390°C) [15].

**Table 11.** The parameters used for x1.2 scale dental implant printed with the second generation printer of Orion [15].

Parameters	Value
Filament diameter	1.75 mm
Nozzle diameter	0.15 mm
Nozzle temperature	405°C
Chamber temperature	250°C
Plate temperature	250°C
Layer heater	200°C
Printing speed	400 mm/min
Layer thickness	0.05 mm
Slicer	Simplify 3D
Printing time	49m 12s

## 4. Discussion

Maximal bending strength of  $193.33 \pm 7.04$  MPa was obtained using a 0.4 mm nozzle in combination with a nozzle temperature of 430 °C and a printing speed of 10 mm/s, while maximal bending modulus of  $1.476 \pm 0.103$  GPa was obtained using a 0.2 mm nozzle in combination with a nozzle temperature of 430 °C and a printing speed of 15 mm/s. Maximal compression strength of  $87 \pm 1.02$  MPa and elastic modulus of  $2.193 \pm 0.058$  GPa were obtained with 0.6 mm nozzle, under the condition of 440 °C, 10 mm/s and 420 °C, 10 mm/s, respectively.

Samples of extruded unfilled PEEK materials subjected to three-point bending tests showed bending strengths of  $170 \pm 19.31$  MPa (VESTAKEEP® M4 R, Evonik Industries, Essen, Germany) and  $182.91 \pm 12.59$  MPa (PEEK Optima LT1, Invibio Ltd., Thornton Cleveleys, UK) and bending modulus of  $2.85 \pm 0.41$  GPa and  $2.73 \pm 0.26$  GPa, respectively [29]. When subjected to compression in the shape of cylinders with a diameter of 5 mm, these materials showed a compressive strength of  $122.85 \pm 0.59$  MPa (VESTAKEEP® M4 R) and  $136.94 \pm 1.01$  MPa (PEEK Optima LT1) as well as an elastic modulus of  $3.04 \pm 0.07$  GPa and  $3.18 \pm 0.02$  GPa, respectively [30]. Compared to the mechanical properties of the printed specimens of the present study, the 3D printed bars showed similar bending strengths, while their bending modulus were about 50 % less than the bars of extruded PEEK. The 3D printed cylinders achieved about 70 % of the compression strength and elastic modulus of the cylinders of extruded PEEK. It must be assumed that the 3D printed test specimens had anisotropic mechanical properties based on the printing system. That means that due to the potential risk of delamination at the layer interfaces under loading, the test specimens would have shown different mechanical properties under different loading directions with regard to the arrangement of the layers. Due to the layer-by-layer application in the z-axis, samples would show the highest mechanical properties when loaded along the z-axis, e.g. in the case of the samples of the present study, and the lowest when loaded along the x- and y- axis [31]. Therefore, a 5-axis printing system allowing an even alignment of the layers in all dimensions would help to achieve isotropic mechanical properties.

In the bending and compression tests, the nozzle diameter was the most significant parameter affecting the final performances of the printed parts. The possible reasons might reside in,

1. Nozzle diameter affects the mechanical properties physically because of different printing routines of the samples. The width of the extruded threads is indirectly defined by the set nozzle size, but slicers allow to define some corrections to these preset configurations

[16][31].

2. The internal defects of the samples vary from each other in different diameter of nozzle. The bending modulus of the samples printed with 0.2 mm and 0.6 mm nozzles were higher while the bending strength was poorer than 0.4 mm nozzle groups, indicating that 0.2 mm and 0.6 mm nozzle were favourable choices for better bending modulus. However, possible structure and internal defects or micro-bubbles could have affected the bending strength of these samples.

The printing speed was the secondary significant parameter affecting the bending strength, the bending modulus and the compression strength. Decreasing the printing speed was more significant to improve the bending strength of the samples printed with a 0.6 mm nozzle than a 0.4 mm nozzle, and did not affect the 0.2 mm nozzle group much. The reason might reside in the feed rate limited by the compression on the liquefier side of the feed rollers [16]. When increasing the printing speed, the feed rate would have enhanced to compensate for the volume of the material extruded from the nozzle. However, the feeding rate might have reached a limit for the 0.2 mm nozzle within the printing speed range of 5 – 15 mm/s because of the obstruction of the narrow outlet, and therefore limited the quality improvement of the products. For the bending modulus, the variance in printing speed had greater influences on samples printed with a 0.2 mm nozzle, and a printing speed of 10 mm/s was not favorable when applying a 0.2 mm nozzle. This indicates that the samples produced with a 0.2 mm nozzle were more likely to produce structure defects. In the experiment, we also noticed that a smaller nozzle such as 0.2 mm became more vulnerable to obstructions in the nozzle outlet due to contaminants introduced within the material or during the printing process, so that the printing speed needs to be chosen carefully. To achieve higher compression strength of the printed parts, a slower printing speed was more beneficial. The reason might be clusters of pore pockets located more within the samples while printing at a faster speed. As for the elastic modulus, increasing the printing speed led to a decrease in elastic modulus at the temperature of 420 °C. On the other hand, a faster printing speed helped to increase the elastic modulus at the temperature of 440 °C. This could be related to the high viscosity of the PEEK material. Wang et al. [32] investigated PEEK within the nozzle's flow channel in a finite element analysis (FEA) to evaluate the influence of the printing temperature. The results showed that a higher temperature in combination with a slower feeding speed extended the length of the liquid PEEK column within the nozzle. At a temperature of 420 °C, the viscosity of the material in the nozzle channel was high, and a faster printing speed would increase the risk of random formation of air gaps and



micro bubbles in the specimens and inconsistency in solidification of the material upon deposition. However, at 440 °C the PEEK in the channel had sufficiently easy flow, and a faster printing speed would decrease printing time, and increase bonding between layers [33].

The nozzle temperature affected the density of samples as well as the mechanical performance, especially the elastic modulus. As a semi-crystalline thermoplastic polymer, PEEK consists of crystalline and amorphous domains. Within the crystalline regions, the macromolecular chains align in higher order and have stronger intermolecular forces, which cause higher strength and rigidity [34]. Conversely, the macromolecules within the amorphous regions tend to intertwine loosely, thus showing a high flexibility [34]. PEEK density could vary between 1.263 g/cm<sup>3</sup> and 1.400 g/ml depending on different crystalline/ amorphous ratio, and PEEK can be up to about 40 % crystalline, though 30- 35 % is more typical [28]. Samples with a higher amount of crystalline domains usually exhibit higher density and stronger mechanical performance. In the present study, the applied temperature was between 420 °C and 440 °C, which were chosen according to pre-test of this brand of filament. Different printing temperature for other brands of PEEK were also reported, of which the reason lies in the purity of the filaments [15]. Samples printed at 420 °C exhibited higher elastic modulus than specimens printed with a nozzle temperature of 440 °C, indicating that the samples formed more crystalline areas when printed at 420 °C. Yang et al. [17] found that nozzle temperature strongly influences crystallinity and mechanical properties of PEEK, because nozzle temperature can influence the crystal melting process, the crystallization process, the interface between printing lines, and the deterioration phenomenon of polymer materials. Regarding Yang et al.'s research, the decrease of the crystalline proportion due to temperature increase can be explained as an incomplete melting of crystalline regions in the nozzle with a lower and non-uniform temperature inside.

To sum up, a combination of a nozzle diameter of 0.4 mm, a nozzle temperature of 430 °C and a printing speed of 5 mm/s were beneficial to get the highest density and bending strength considering the printed samples under these conditions showed the least defects. To obtain a better bending modulus, a 0.2 mm nozzle should be used, and a higher nozzle temperature of 440 °C as well as slower printing speed reduced possible internal defects. The most compact cylinders and the best compression properties can be achieved with a 0.6 mm nozzle.

As for the dimension accuracy, the least accurate width and the most accurate diameter were obtained with a 0.4 mm nozzle. A wider nozzle would have caused fewer lines on the x-y plane, so that the effect of die swell and the correction of the slicer of overlapping or gapping would

happen less frequently thus causing a smaller error. And the print sequence between the wall and infill can also influence the shape of print part and the quantity of the wall also can change the accuracy of the shape of samples. What’s more, the printing speed influenced the accuracy as well. When printing at a lower speed, the extruded material would have been exposed to the heat of the nozzle for a longer time, which would have melted the material sufficiently resulting in lower viscosity. When printing straight lines, the influence of extra heat was of secondary concern because the nozzle was moving in a relatively wider distance; however, when printing round lines such as the contour and infill lines of the cylinders, the nozzle was moving within a small area, so the factors slicer and thermodynamics of PEEK should be taken into consideration. A 0.6 mm nozzle might have resulted in higher accuracy because of less errors caused by the slicer algorithm; a 0.4 mm nozzle together with a printing speed of 10 mm/s would be beneficial to obtain more accurate dimensions, which might be because the thermal property of extruded material and the algorithm of the slicer strike a balance under this condition.

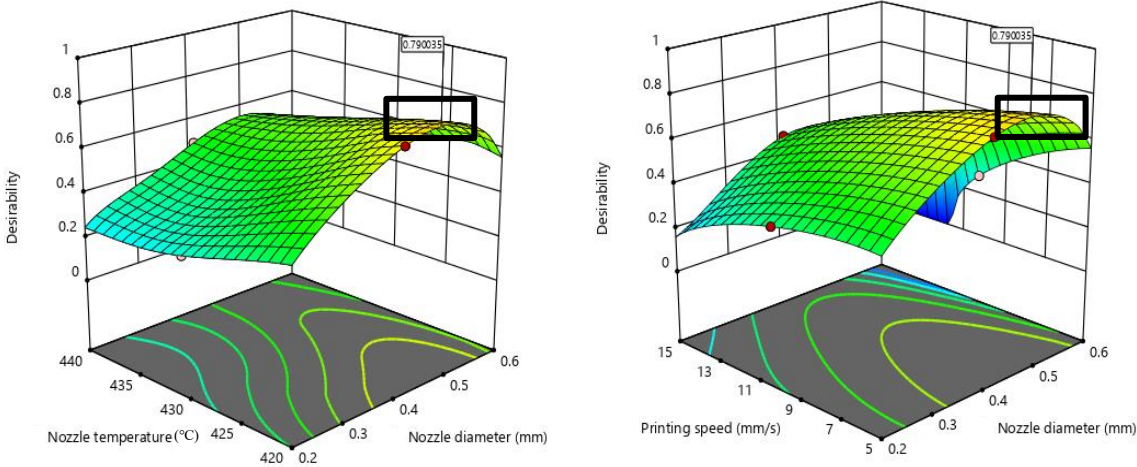


**Figure 17.** The optimized parameters for maximal bending strength and elastic modulus assuming these two parameters are of the same importance (within the black square are the most desirable combinations).

The tensile strength of printed parts along the vertical printing plane is usually far less than the compressive strength, consequently products made from additive manufacturing are more suitable to be used in conditions to withstand compressive stress, such as spine cages and dental implants. In the case of 3D printed dental implants, the bending strength vertical to the x-y plane and the elastic modulus along with the z-axis are the most important issues related to this

particular application. The most favourable parameter combinations value areas are shown in Figure 17, which are close to the combination of a nozzle diameter of 0.5 mm, a nozzle temperature of 420 °C and a printing speed of 5 mm/s.

As for the designed shape of dental implants, regarding the hollow cylinders compared to the solid cylinders with a cross sectional area of 12.566 mm<sup>2</sup>, the elastic modulus was reduced by 14 % and 28 % for the specimens with a wall thickness of 1.2 mm (cross sectional area: 10.555 mm<sup>2</sup>) and 0.6 mm (cross sectional area: 6.158 mm<sup>2</sup>), respectively, whereas their cross sectional areas for the applied forces were reduced by 16 % and 49% compared to the solid cylinder, respectively. Reducing the cross sectional area with outer threads, reduced the elastic modulus by 16 % compared to the solid cylinder, whereas the cross sectional area of the core amounted 6.947 mm<sup>2</sup> and was reduced by 55 % compared to the solid cylinder. The possibility of post-processing methods such as annealing or plasma on the surface of PEEK devices could also be taken into consideration in the future. Additionally, the compression- shear test and torsion test are worthy to be conducted, as well as fatigue loading tests to simulate chewing forces.

## 5. Conclusions and clinical implications

Patient-orientated therapy model is now drawing efforts to precisely manufactured dental devices and attachment in dentistry field. 3D printing is with no doubt an alternative way to accomplish this goal. Considering the great mechanical properties and reliable biocompatibility of PEEK, it has great potential to be used as substitute of medical devices, and 3D printing strategy offers a promising way of process production and manufacture.

Knowing that for these tests not the last developed machine was used, we could demonstrate the limits, which drive us to the conclusion that it is necessary to adjust following parameters:

1. Statistical analysis indicated that nozzle diameter was the most influential parameter on the mechanical properties of printed PEEK parts, among the three printing parameters chosen in our experiment related with FDM strategy, followed by printing speed and nozzle temperature.
2. A combination of 0.4mm nozzle diameter, 430 °C nozzle temperature and printing speed of 5mm/s is beneficial to get the best bending strength; 0.2mm nozzle is recommended for better bending modulus, a higher nozzle temperature and slower printing speed is favorable to reduce possible internal defects. Meanwhile, the best compression property can be achieved with 0.6mm nozzle or even wider nozzles. However, wider nozzle diameter improved elastic modulus of samples, which is the most concerned index for dental implant, but led to deterioration of appearance quality.
3. Good mechanical properties and fine microstructure of dental implant made from PEEK were obtained by FDM strategy. The most popular design for titanium implants such as hole inside the bulk or screw on the surface would decrease the elastic modulus however matches well with the alveolar bone.
4. More efforts to optimize the performance of printed dental implants based on PEEK and its compounds still worth exploring.

Until now, printing of reproducible tiny sized PEEK parts has proved to be possible in our experiments, which is achieved through optimization of the FDM printing parameters. There is still long way as to accomplish the transition from research phase to 3D printed PEEK manufacturing, and finally reach the goal of integrating the treatment within clinic. However, this trial might lay a basis for the patient- specialized treatment in the field of dental implantology. Considering the complexity of chewing forces, systematical mechanical tests are needed, simulation based on finite element analysis is necessary in the further research.

## 6. Reference

- [1] S. Şahin, M.C. Çehreli, E. Yalçın, The influence of functional forces on the biomechanics of implant-supported prostheses - A review, *J. Dent.* 30 (2002) 271–282.  
[https://doi.org/10.1016/S0300-5712\(02\)00065-9](https://doi.org/10.1016/S0300-5712(02)00065-9).
- [2] A. Sicilia, S. Cuesta, G. Coma, I. Arregui, C. Guisasola, E. Ruiz, A. Maestro, Titanium allergy in dental implant patients: A clinical study on 1500 consecutive patients, *Clin. Oral Implants Res.* 19 (2008) 823–835. <https://doi.org/10.1111/j.1600-0501.2008.01544.x>.
- [3] H. Egusa, N. Ko, T. Shimazu, H. Yatani, Suspected association of an allergic reaction with titanium dental implants: A clinical report, *J. Prosthet. Dent.* 100 (2008) 344–347.  
[https://doi.org/10.1016/S0022-3913\(08\)60233-4](https://doi.org/10.1016/S0022-3913(08)60233-4).
- [4] L. Gremillard, L. Martin, L. Zych, E. Crosnier, J. Chevalier, A. Charbouillot, P. Sainsot, J. Espinouse, J.L. Aurelle, Combining ageing and wear to assess the durability of zirconia-based ceramic heads for total hip arthroplasty, *Acta Biomater.* 9 (2013) 7545–7555. <https://doi.org/10.1016/j.actbio.2013.03.030>.
- [5] A. Schwitalla, W.D. Müller, PEEK dental implants: A review of the literature, *J. Oral Implantol.* 39 (2013) 743–749. <https://doi.org/10.1563/AAID-JOI-D-11-00002>.
- [6] K. Liao, Performance Characterization and Modeling of a Composite Hip Prosthesis, *Exp. Tech.* 18 (1994) 33–38. <https://doi.org/10.1111/j.1747-1567.1994.tb00303.x>.
- [7] G.R. Maharaj, R.D. Jamison, Intraoperative impact: Characterization and laboratory simulation on composite hip prostheses, *ASTM Spec. Tech. Publ.* (1993) 98–108.  
<https://doi.org/10.1520/stp15546s>.
- [8] S.M. Kurtz, J.N. Devine, PEEK biomaterials in trauma, orthopedic, and spinal implants, *Biomaterials.* 28 (2007) 4845–4869. <https://doi.org/10.1016/j.biomaterials.2007.07.013>.
- [9] D.J. Kelsey, G.S. Springer, S.B. Goodman, Composite implant for bone replacement, *J. Compos. Mater.* 31 (1997) 1593–1632. <https://doi.org/10.1177/002199839703101603>.
- [10] S.M. Kurtz, An Overview of PEEK Biomaterials, in: *PEEK Biomater. Handb.*, Elsevier Inc., (2012) pp. 3-9.  
<https://doi.org/10.1016/B978-1-4377-4463-7.10001-6>.
- [11] S.X. Lu, P. Cebe, M. Capel, Thermal stability and thermal expansion studies of PEEK and related polyimides, *Polymer (Guildf).* 37 (1996) 2999–3009.  
[https://doi.org/10.1016/0032-3861\(96\)89397-9](https://doi.org/10.1016/0032-3861(96)89397-9).

- [12] S.M. Kurtz, Synthesis and Processing of PEEK for Surgical Implants, in: PEEK Biomater. Handb., Elsevier Inc., (2012) pp. 9–22.  
<https://doi.org/10.1016/B978-1-4377-4463-7.10002-8>.
- [13] M. Schmidt, D. Pohle, T. Rechtenwald, Selective laser sintering of PEEK, CIRP Ann. - Manuf. Technol. 56 (2007) 205–208. <https://doi.org/10.1016/j.cirp.2007.05.097>.
- [14] C.U. Lee, J. Vandenbrande, A.E. Goetz, M.A. Ganter, D.W. Storti, A.J. Boydston, Room temperature extrusion 3D printing of polyether ether ketone using a stimuli-responsive binder, Addit. Manuf. 28 (2019) 430–438. <https://doi.org/10.1016/j.addma.2019.05.008>.
- [15] Y. Wang, W.D. Müller, A. Rumjahn, A. Schwitalla, Parameters influencing the outcome of additive manufacturing of tiny medical devices based on PEEK, Materials (Basel). 13 (2020) 1–15. <https://doi.org/10.3390/ma13020466>.
- [16] B.N. Turner, R. Strong, S.A. Gold, A review of melt extrusion additive manufacturing processes: I. Process design and modeling, Rapid Prototyp. J. 20 (2014) 192–204.  
<https://doi.org/10.1108/RPJ-01-2013-0012>.
- [17] C. Yang, X. Tian, D. Li, Y. Cao, F. Zhao, C. Shi, Influence of thermal processing conditions in 3D printing on the crystallinity and mechanical properties of PEEK material, J. Mater. Process. Technol. 248 (2017) 1–7.  
<https://doi.org/10.1016/j.jmatprotec.2017.04.027>.
- [18] W. Wu, P. Geng, G. Li, D. Zhao, H. Zhang, J. Zhao, Influence of layer thickness and raster angle on the mechanical properties of 3D-printed PEEK and a comparative mechanical study between PEEK and ABS, Materials (Basel). 8 (2015) 5834–5846.  
<https://doi.org/10.3390/ma8095271>.
- [19] X. Deng, Z. Zeng, B. Peng, S. Yan, W. Ke, Mechanical properties optimization of poly-ether-ether-ketone via fused deposition modeling, Materials (Basel). 11 (2018) 1–11.  
<https://doi.org/10.3390/ma11020216>.
- [20] P. Geng, J. Zhao, W. Wu, W. Ye, Y. Wang, S. Wang, S. Zhang, Effects of extrusion speed and printing speed on the 3D printing stability of extruded PEEK filament, J. Manuf. Process. 37 (2019) 266–273. <https://doi.org/10.1016/j.jmapro.2018.11.023>.
- [21] B. Hu, X. Duan, Z. Xing, Z. Xu, C. Du, H. Zhou, R. Chen, B. Shan, Improved design of fused deposition modeling equipment for 3D printing of high-performance PEEK parts, Mech. Mater. 137 (2019) 103139. <https://doi.org/10.1016/j.mechmat.2019.103139>.
- [22] M. Vaezi, S. Yang, Extrusion-based additive manufacturing of PEEK for biomedical applications, Virtual Phys. Prototyp. 10 (2015) 123–135.  
<https://doi.org/10.1080/17452759.2015.1097053>.

- [23] K.M. Rahman, T. Letcher, R. Reese, Mechanical properties of additively manufactured peek components using fused filament fabrication, *ASME Int. Mech. Eng. Congr. Expo. Proc.* 2A-2015 (2015) V02AT02A009. <https://doi.org/10.1115/IMECE2015-52209>.
- [24] S. Berretta, R. Davies, Y.T. Shyng, Y. Wang, O. Ghita, Fused Deposition Modelling of high temperature polymers: Exploring CNT PEEK composites, *Polym. Test.* 63 (2017) 251–262. <https://doi.org/10.1016/j.polymertesting.2017.08.024>.
- [25] G. Cicala, A. Latteri, B. Del Curto, A. Lo Russo, G. Recca, S. Farè, Engineering thermoplastics for additive manufacturing: A critical perspective with experimental evidence to support functional applications, *J. Appl. Biomater. Funct. Mater.* 15 (2017) e10–e18. <https://doi.org/10.5301/jabfm.5000343>.
- [26] X. Han, D. Yang, C. Yang, S. Spintzyk, L. Scheideler, P. Li, D. Li, J. Geis-Gerstorfer, F. Rupp, Carbon Fiber Reinforced PEEK Composites Based on 3D-Printing Technology for Orthopedic and Dental Applications, *J. Clin. Med.* 8 (2019) 240. <https://doi.org/10.3390/jcm8020240>.
- [27] Q. Li, W. Zhao, Y. Li, W. Yang, G. Wang, Flexural properties and fracture behavior of CF/PEEK in orthogonal building orientation by FDM: Microstructure and mechanism, *Polymers (Basel)*. 11 (2019) 1–15. <https://doi.org/10.3390/polym11040656>.
- [28] M. Reitman, D. Jaekel, R. Siskey, S.M. Kurtz, *Morphology and Crystalline Architecture of Polyaryletherketones*, Elsevier Inc., 2012. <https://doi.org/10.1016/B978-1-4377-4463-7.10004-1>.
- [29] A.D. Schwitalla, T. Spintig, I. Kallage, W.D. Müller, Flexural behavior of PEEK materials for dental application, *Dent. Mater.* 31 (2015) 1377–1384. <https://doi.org/10.1016/j.dental.2015.08.151>.
- [30] A.D. Schwitalla, T. Spintig, I. Kallage, W.D. Müller, Pressure behavior of different PEEK materials for dental implants, *J. Mech. Behav. Biomed. Mater.* 54 (2016) 295–304. <https://doi.org/10.1016/j.jmbbm.2015.10.003>.
- [31] A.R. Torrado, C.M. Shemelya, J.D. English, Y. Lin, R.B. Wicker, D.A. Roberson, Characterizing the effect of additives to ABS on the mechanical property anisotropy of specimens fabricated by material extrusion 3D printing, *Addit. Manuf.* 6 (2015) 16–29. <https://doi.org/10.1016/j.addma.2015.02.001>.
- [32] P. Wang, B. Zou, H. Xiao, S. Ding, C. Huang, Effects of printing parameters of fused deposition modeling on mechanical properties, surface quality, and microstructure of PEEK, *J. Mater. Process. Technol.* 271 (2019) 62–74. <https://doi.org/10.1016/j.jmatprotec.2019.03.016>.

- [33] C. Basgul, T. Yu, D.W. MacDonald, R. Siskey, M. Marcolongo, S.M. Kurtz, Does annealing improve the interlayer adhesion and structural integrity of FFF 3D printed PEEK lumbar spinal cages?, *J. Mech. Behav. Biomed. Mater.* 102 (2020) 103455. <https://doi.org/10.1016/j.jmbbm.2019.103455>.
- [34] J.E. Mark, Part VII. Crystallinity and morphology, in *Physical Properties of Polymers Handbook.*, Springer Inc., (2007) pp. 611-715. <https://doi.org/10.1007/978-0-387-69002-5>.



## Statutory Declaration

“I, Yiqiao, Wang, by personally signing this document in lieu of an oath, hereby affirm that I prepared the submitted dissertation on the topic: **“Evaluation of process parameters for the manufacture of tiny biomedical devices via 3D printing of PEEK/ Auswertung von Prozessparametern zur Herstellung winziger biomedizinischer Geräte mittels 3D-Druck von PEEK”**, independently and without the support of third parties, and that I used no other sources and aids than those stated.

All parts which are based on the publications or presentations of other authors, either in letter or in spirit, are specified as such in accordance with the citing guidelines. The sections on methodology (in particular regarding practical work, laboratory regulations, statistical processing) and results (in particular regarding figures, charts and tables) are exclusively my responsibility.

My contributions to any publications to this dissertation correspond to those stated in the below joint declaration made together with the supervisor. All publications created within the scope of the dissertation comply with the guidelines of the ICMJE (International Committee of Medical Journal Editors; [www.icmje.org](http://www.icmje.org)) on authorship. In addition, I declare that I shall comply with the regulations of Charité– Universitätsmedizin Berlin on ensuring good scientific practice.

I declare that I have not yet submitted this dissertation in identical or similar form to another Faculty.

The significance of this statutory declaration and the consequences of a false statutory declaration under criminal law (Sections 156, 161 of the German Criminal Code) are known to me.”

Date

Signature

## **Declaration of Your Own Contribution to the Publications**

Yiqiao Wang, Wolf Dieter Müller, Adam Rumjahn, Andreas Schwitalla\*. Parameters Influencing the Outcome of Additive Manufacturing of Tiny Medical Devices Based on PEEK [J]. *Materials (Basel)*, 2020, 13(2), 466

Yiqiao Wang elaborated the essential parts of the concept and design of this systematic review and then came out with the experiment plan. She performed the literature search, extracted the study results, and summarized the data in Table 1-3, Figure 3 and schematic diagram (Figure 1-2) shown in the paper. She also conducted the experiment in the last part of the review with support from Adam Rumjahn, and documented as Figures 4-7 and parameters list (Table 4-5). She presented all the data and critical analyses in the working group. Prof. Dr. Müller together with Dr. Schwitalla controlled the correctness and plausibility of extracted data. Finally, Yiqiao Wang drafted the concept for this paper and wrote the manuscript independently after the draft was accepted in the discussion round of the working group. During the journal submission procedure, Yiqiao Wang responded to the reviewers' questions after discussion within group and made essential supplement to the manuscript.

---

Signature, date and stamp of first supervising university professor / lecturer

---

Signature of doctoral candidate

## Extract from the Journal Summary List

Journal Data Filtered By: **Selected JCR Year: 2018** Selected Editions: SCIE,SSCI  
 Selected Categories: **"MATERIALS SCIENCE, MULTIDISCIPLINARY"**  
 Selected Category Scheme: WoS  
**Gesamtanzahl: 293 Journale**

Rank	Full Journal Title	Total Cites	Journal Impact Factor	Eigenfactor Score
1	Nature Reviews Materials	7,901	74.449	0.033870
2	Nature Energy	11,113	54.000	0.040630
3	NATURE MATERIALS	97,792	38.887	0.177380
4	Nature Nanotechnology	63,245	33.407	0.154960
5	ADVANCED MATERIALS	229,186	25.809	0.409390
6	Advanced Energy Materials	50,724	24.884	0.120610
7	Materials Today	12,566	24.372	0.018830
8	PROGRESS IN MATERIALS SCIENCE	14,580	23.725	0.016820
9	MATERIALS SCIENCE & ENGINEERING R-REPORTS	7,206	22.250	0.006250
10	INTERNATIONAL MATERIALS REVIEWS	5,262	21.086	0.004960
11	Annual Review of Materials Research	8,086	16.816	0.007830
12	Nano Today	7,980	16.582	0.012950
13	ACS Energy Letters	10,134	16.331	0.031350
14	Advanced Science	8,129	15.804	0.021030
15	ADVANCED FUNCTIONAL MATERIALS	95,431	15.621	0.175970
16	Nano Energy	37,106	15.548	0.087250
17	Materials Horizons	4,587	14.356	0.013710
18	ACS Nano	152,659	13.903	0.325710
19	NANO LETTERS	163,570	12.279	0.300620
20	Small	49,968	10.856	0.091450
21	Journal of Materials Chemistry A	126,338	10.733	0.295190

Rank	Full Journal Title	Total Cites	Journal Impact Factor	Eigenfactor Score
22	CHEMISTRY OF MATERIALS	106,568	10.159	0.150260
23	npj Computational Materials	954	9.200	0.003660
24	Nanoscale Horizons	888	9.095	0.002340
25	Nano-Micro Letters	2,209	9.043	0.003590
26	Nano Research	16,517	8.515	0.031810
27	ACS Applied Materials & Interfaces	170,096	8.456	0.366360
28	CURRENT OPINION IN SOLID STATE & MATERIALS SCIENCE	3,955	8.418	0.004700
29	NPG Asia Materials	4,387	8.052	0.011090
30	Applied Materials Today	1,608	8.013	0.003470
31	PROGRESS IN PHOTOVOLTAICS	8,325	7.776	0.011390
32	JOURNAL OF POWER SOURCES	116,432	7.467	0.134510
33	CARBON	74,892	7.466	0.085220
34	Materials Research Letters	1,564	7.440	0.005230
35	2D Materials	5,487	7.343	0.022810
36	Journal of Physical Chemistry Letters	45,404	7.329	0.124340
37	ACTA MATERIALIA	73,990	7.293	0.090910
38	Additive Manufacturing	2,445	7.173	0.005200
39	ACS Photonics	9,956	7.143	0.033670
40	Advanced Optical Materials	8,586	7.125	0.026060
41	Nanoscale	92,732	6.970	0.208040
42	Nanophotonics	1,936	6.908	0.006090
43	Virtual and Physical Prototyping	993	6.825	0.001870

Selected JCR Year: 2018; Selected Categories: "MATERIALS SCIENCE, MULTIDISCIPLINARY"

Rank	Full Journal Title	Total Cites	Journal Impact Factor	Eigenfactor Score
44	Journal of Materials Chemistry C	40,067	6.641	0.097440
45	CRITICAL REVIEWS IN SOLID STATE AND MATERIALS SCIENCES	1,475	6.455	0.001690
46	CORROSION SCIENCE	37,952	6.355	0.028720
47	Advanced Electronic Materials	3,886	6.312	0.011930
48	SOLAR ENERGY MATERIALS AND SOLAR CELLS	30,400	6.019	0.031820
49	INTERNATIONAL JOURNAL OF PLASTICITY	11,299	5.800	0.013670
50	MATERIALS & DESIGN	53,840	5.770	0.089000
51	Science China-Materials	1,878	5.636	0.003590
52	CEMENT AND CONCRETE RESEARCH	34,278	5.618	0.016250
53	Advanced Materials Technologies	1,429	5.395	0.003380
54	JOURNAL OF MATERIALS SCIENCE & TECHNOLOGY	6,753	5.040	0.009080
55	Sustainable Energy & Fuels	1,344	4.912	0.002650
56	IUCrJ	1,363	4.756	0.006430
57	Advanced Materials Interfaces	6,238	4.713	0.016510
58	MRS BULLETIN	7,862	4.655	0.010250
59	SCRIPTA MATERIALIA	33,032	4.539	0.033680
60	Journal of Physical Chemistry C	149,348	4.309	0.216950
61	APL Materials	4,061	4.296	0.014770
62	PARTICLE & PARTICLE SYSTEMS CHARACTERIZATION	3,379	4.194	0.006390
63	MICROPOROUS AND MESOPOROUS MATERIALS	25,303	4.182	0.024180
64	JOURNAL OF MATERIALS PROCESSING TECHNOLOGY	33,606	4.178	0.021130
65	JOURNAL OF ALLOYS AND COMPOUNDS	102,817	4.175	0.131760

Rank	Full Journal Title	Total Cites	Journal Impact Factor	Eigenfactor Score
66	CRYSTAL GROWTH & DESIGN	29,940	4.153	0.037860
67	JOURNAL OF THE MECHANICS AND PHYSICS OF SOLIDS	18,866	4.087	0.019250
68	MATERIALS SCIENCE AND ENGINEERING A-STRUCTURAL MATERIALS PROPERTIES MICROSTRUCTURE AND PROCESSING	79,492	4.081	0.065810
69	Extreme Mechanics Letters	1,439	4.075	0.005890
70	CONSTRUCTION AND BUILDING MATERIALS	56,987	4.046	0.063710
71	Nanomaterials	4,955	4.034	0.008390
72	Liquid Crystals Reviews	176	3.917	0.000810
73	APPLIED CLAY SCIENCE	15,784	3.890	0.014850
74	PHYSICAL REVIEW B	371,919	3.736	0.363380
75	Physica Status Solidi-Rapid Research Letters	3,346	3.729	0.008100
76	LANGMUIR	117,927	3.683	0.096010
77	INTERNATIONAL JOURNAL OF FATIGUE	13,715	3.673	0.014320
78	SCIENCE AND TECHNOLOGY OF ADVANCED MATERIALS	5,047	3.585	0.005870
79	Smart Materials and Structures	19,870	3.543	0.025150
80	Materials Science and Engineering B-Advanced Functional Solid-State Materials	10,565	3.507	0.005690
81	ORGANIC ELECTRONICS	12,429	3.495	0.018640
82	JOURNAL OF MATERIALS SCIENCE	50,817	3.442	0.034620
83	NANOTECHNOLOGY	43,992	3.399	0.048160
83	Soft Matter	36,016	3.399	0.066600
85	IEEE Journal of Photovoltaics	4,887	3.398	0.011360

Rank	Full Journal Title	Total Cites	Journal Impact Factor	Eigenfactor Score
86	ChemNanoMat	1,249	3.379	0.003310
87	MATERIALS RESEARCH BULLETIN	21,620	3.355	0.018260
88	INTERMETALLICS	10,599	3.353	0.010410
89	MATERIALS AND MANUFACTURING PROCESSES	5,749	3.350	0.005230
90	Journal of Materials Research and Technology-JMR&T	1,327	3.327	0.002420
91	Nano Convergence	461	3.324	0.001220
92	Progress in Natural Science-Materials International	4,119	3.310	0.004270
93	3D Printing and Additive Manufacturing	505	3.259	0.001280
94	MATERIALS CHARACTERIZATION	11,421	3.220	0.016140
95	Nanoscale Research Letters	16,143	3.159	0.023390
96	International Journal of Mechanics and Materials in Design	800	3.143	0.001220
97	LIQUID CRYSTALS	5,589	3.078	0.004380
98	Results in Physics	3,539	3.042	0.004650
99	MACROMOLECULAR MATERIALS AND ENGINEERING	5,400	3.038	0.005180
100	CMC-Computers Materials & Continua	611	3.024	0.000400
101	MATERIALS LETTERS	46,192	3.019	0.049070
102	Materials	18,764	2.972	0.030940
103	MECHANICS OF MATERIALS	7,353	2.958	0.008250
104	WEAR	27,268	2.950	0.016150
105	Physical Review Materials	1,584	2.926	0.004750
105	Plasmonics	3,701	2.926	0.006180
107	ADVANCED ENGINEERING MATERIALS	8,426	2.906	0.009140

Selected JCR Year: 2018; Selected Categories: "MATERIALS SCIENCE, MULTIDISCIPLINARY"

## Printed Copy of the Publication

Parameters Influencing the Outcome of Additive Manufacturing of  
Tiny Medical Devices Based on PEEK

Yiqiao Wang\*, Wolf-Dieter Müller, Adam Rumjahn and Andreas Schwitalla

\* Yiqiao Wang is the first author of the publication

Wang, Yiqiao, Wolf-dieter Müller, Adam Rumjahn, and Andreas Schwitalla. 2020. “Parameters Influencing the Outcome of Additive Manufacturing of Tiny Medical Devices Based on PEEK.”


*Materials* 2020, 13(2), 466.

<https://doi.org/10.3390/ma13020466>



Review

# Parameters Influencing the Outcome of Additive Manufacturing of Tiny Medical Devices Based on PEEK

Yiqiao Wang <sup>1</sup> , Wolf-Dieter Müller <sup>1</sup>, Adam Rumjahn <sup>2</sup> and Andreas Schwitalla <sup>1,\*</sup>

<sup>1</sup> Dental Materials and Biomaterial Research, Department of Prosthodontics, School of Dentistry, Charité-University Medicine Berlin, Aßmannshäuser Str. 4–6, 14197 Berlin, Germany; wangyq0621@sina.com (Y.W.); wolf-dieter.mueller@charite.de (W.-D.M.)

<sup>2</sup> Orion Additive Manufacturing GmbH, Gustav-Meyer-Allee 25, 13355 Berlin, Germany; adam@orion-am.com

\* Correspondence: andreas.schwitalla@charite.de

Received: 1 December 2019; Accepted: 14 January 2020; Published: 18 January 2020



**Abstract:** In this review, we discuss the parameters of fused deposition modeling (FDM) technology used in finished parts made from polyether ether ketone (PEEK) and also the possibility of printing small PEEK parts. The published articles reporting on 3D printed PEEK implants were obtained using PubMed and search engines such as Google Scholar including references cited therein. The results indicate that although many have been experiments conducted on PEEK 3D printing, the consensus on a suitable printing parameter combination has not been reached and optimized parameters for printing worth pursuing. The printing of reproducible tiny-sized PEEK parts with high accuracy has proved to be possible in our experiments. Understanding the relationships among material properties, design parameters, and the ultimate performance of finished objects will be the basis for further improvement of the quality of 3D printed medical devices based on PEEK and to expand the polymers applications.

**Keywords:** PEEK; fused deposition modeling (FDM); printing parameters; mechanical characteristics; medical devices

## 1. Introduction

Polyether ether ketone (PEEK) is one of the most important members of the polyaromatic ether ketone (PAEKs), which is a family of high-performance thermoplastic polymers, consisting of an aromatic backbone molecular chain, interconnected by ketone and ether functional groups [1,2]. The molecular structures of PAEKs contain rigid benzene rings, which makes them resistant to high temperature and chemical attacks. Meanwhile, the ether bonds in the molecular backbone of polyether ketones are responsible for the flexibility of the polymers, giving them the possibility to be processed [2,3]. PEEK owns a melting point ( $T_m$ ) of 343 °C and the glass transition temperature ( $T_g$ ) of 143 °C and shows excellent mechanical properties including high strength, elastic modulus, and fracture toughness. PEEK is generally considered a high-performance thermoplastic polymer [4], and is getting increasing attention in the medical field. PEEK was commercialized by the UK company Invibio as a biomaterial for implants in 1998 because it can resist degradation *in vivo* [5]. Being considered as the leading thermoplastic candidate for replacing metal implant components, PEEK parts such as spine cages and retaining rings for acetabular cup assembly especially have potential in orthopedics [3,6,7] and trauma [8] due to its cortical bone-like elastic modulus.

Many techniques are used for the production of porous PEEK for medical applications. Traditional manufacturing process methods include injection molding, extrusion, compression molding, machining,

and so on [9]. Additionally, advancements in additive manufacturing (AM) continue to provide new opportunities for biomedical applications by enabling the creation of more complex architectures, e.g., for tissue engineering scaffolding and patient-personalized implants. The selective laser sintering (SLS) technique was used a decade ago in PEEK 3D printing, which is a type of powder-based AM technology. It is capable of fabricating porous PEEK-based composites with very complex architectures, permitting greater freedom of design [10]. Both 3D systems and EOS have commercialized PEEK in their SLS machines. However, the high cost and concentrated laser beam restrict it from sintering large areas or laminates. Another power-based technique is also applied in PEEK printing. In 2019, Lee et al. [11] reported their efforts toward 3D printing of PEEK by direct-ink writing technology at room temperature, which was enabled by a unique formulation comprised of commercial PEEK powder, soluble epoxy-functionalized PEEK (ePEEK), and fenchone. This combination formed a Bingham plastic that could be extruded using a readily available direct-ink write printer. Besides the techniques mentioned above, fused deposition modeling (FDM) is currently the most widely used 3D printing strategy and low-cost technology for thermoplastic materials [12]. In the FDM process, a filament is extruded from a nozzle continuously while heated to a semiliquid state, then the filament rapidly adheres with the surrounding material and solidifies, and the deposits follow a certain routine to form the desired shape [13]. The schematic of an FDM PEEK printer is showed in Figure 1. Despite a large number of publications on extrusion-based AM of porous structures using other materials than PEEK [14], there are few reports dealing with the AM of small PEEK parts, especially samples without defects such as warpage or delamination.

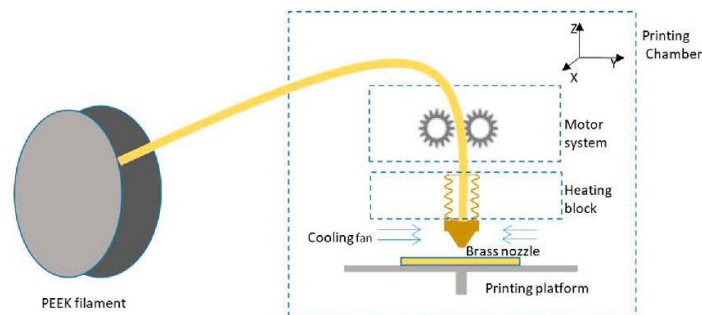


**Figure 1.** Schematic diagram of fused deposition modeling (FDM) 3D polyether ether ketone (PEEK) printer.

In this paper, we will discuss the parameters important for the AM applied to PEEK implants, based on current publications as well as our own research. We highlight the influence of process and design parameters on the performance and mechanical properties of small printed PEEK objects.

## 2. Literature Survey

Literature was obtained using PubMed and search engines such as Google Scholar including references cited therein. All articles included in this review were published within five years before October 2019. We searched for the following terms: “PEEK or Polyether ether ketone” and “3D printing or additive manufacturing” and “parameter”. We excluded review articles, case reports, and articles without detailed information on printing parameters. Only articles in English and that were highly related to PEEK processing parameters using extruded strategy were included.

## 3. Results

Thirteen articles from twelve different authors are included in our review. The detailed parameters applied in the experiments and mechanical properties of printed samples are summarized in Tables 1 and 2.

Table 1. Summary of articles discussing printing parameters and results.

Author	Year of Publication	Materials	Printing System	Parameters	Details	Characterization Techniques
Wu et al. [15]	2014	Unfilled PEEK	Custom-made PEEK 3D printing system	Desiccation	130 °C for 8 h	SEM, 3D scanner
				Nozzle temperature	340 °C–360 °C	
Wu et al. [16]	2015	Unfilled PEEK and ABS plus-TM-P430	Custom-made PEEK 3D printing system	Chamber temperature	90 °C–130 °C	Tensile, bending, and compressive test
				Layer thickness	0.2, 0.3, 0.4 mm	
				Raster angle	0°, 30°, 45°	
Vaezi et al. [17]	2015	PEEK OPTIMA LT3 power (InVivo) and Victrex®/PEEK 450 G filament	Syringe-based and filament-based extrusion system	Desiccation	150 °C for 3 h	Tensile test, three-point flexural test and compressive test
				Nozzle material	Brass and stainless steel	
				Nozzle temperature	350–450 °C	
				Plate temperature	100 °C	
				Ambient temperature	80 °C	
				Layer thickness	0.2 mm	
Rahman et al. [18]	2016	A proprietary PEEK formulation from Arevo Labs	Arevo Labs 3D printer	Nozzle temperature	340 °C	Tensile, compression, flexural, and impact testing
				Platform temperature	230 °C	
				Nozzle diameter	Approx. 0.2 mm	
				Printing speed	50 mm/s	
				Infill ratio	100%	
				Layer height	0.25 mm	
				Raster orientation	0°, 90°	
				Nozzle temperature	360, 380, 400, 420, 440, 460, 480	
				Ambient temperature	25, 50, 100, 150, 200	
				Heat treatment methods	Air cooling, furnace cooling, quenching, annealing, tempering	
Yang et al. [13]	2017	PEEK filament reprocessed from the PEEK pellets (450 G, VICTREX Corp. in UK)	Temperature-control 3D printing system	Other parameters	Nozzle diameter = 0.4 mm; layer thickness = 0.2 mm; printing speed = 40 mm/s; raster angle—consistent with longest edge	Tensile test, DSC
				Desiccation	150 °C for 5 h	
Berretta et al. [19]	2017	PEEK 450, 1% CNT PEEK 450 and 5% CNT PEEK 450 (filaments diameter = 2.7 ± 0.3 mm)	A MandelMax v2.0 (Maker's Tool Works)	Nozzle temperature	350, 365, 380 °C	Tensile test, short beam shear stress test, SEM, TEM, CT, DSC
				Layer height	0.2 mm	

Table 1. Cont.

Author	Year of Publication	Materials	Printing System	Parameters	Details	Characterization Techniques
Deng et al. [20]	2018	PEEK-1000 bar	Custom-built FDM equipment	Printing temperature Layer thickness Printing speed Filling ratio	350–370 °C 0.2, 0.25, 0.3 mm 20, 40, 60 mm/s 20%, 40%, 60%	Tensile, impact and three-point bending test
Cicala et al. [21]	2018	Industrial-grade PEEK (Luvocomm, Hamburg, Germany) and PC	Roboze one 400+ (Roboze, Bari, Italy) Stratasys Fortus@400 mc	Desiccation Other parameters	140 °C for 48 h (pellet) Nozzle temperature = 420 °C; bed temperature = 110 °C; layer height = 0.1 mm; print speed = 20 mm/s; infill = 75%	Tensile test
Geng et al. [22]	2019	PEEK 450 G VICTREX®	Self-made PEEK 3D printing system	Desiccation Nozzle diameter Nozzle temperature Extrusion speed	120 °C for 12 h 0.4, 0.5, 0.6 mm 360 °C 0.1 to 120 mm/min	Surface morphology
Han et al. [23]	2019	Pure PEEK and carbon-fiber-reinforced PEEK (CFR-PEEK)	3D printer (Jugao-AM Tech. Corp. Xian, China)	Surface modification Furnace cooling down Other parameters	Untreated, polished, sandblasted 300 °C for 2 h in furnace then under room temperature Nozzle diameter = 0.4 mm; nozzle temperature = 420 °C; ambient temperature = 20 °C; layer thickness = 0.2 mm; printing speed = 40 mm/s; raster angle—consistent with the longest edge	① Mechanical characterization—tensile, bending, and compressive tests; ② Biological tests—cytotoxicity and cell adhesion test; ③ SEM, surface topography; water contact angle
Hu et al. [24]	2019	PEEK filament (Sting3D Technology Co. Ltd.)	Modified printer from Speedy Maker Company	Raster angle Other parameters	Tensile and bending samples—consistent with longest edge; warpage sample—45° Nozzle temperature = 385 °C; nozzle diameter = 0.4 mm; layer thickness = 0.1 mm; printing speed = 25 mm/s; infill ratio = 100%	Warpage measurement, tensile test, and bending test
Basgul et al. [25]	2019	PEEK OPTIMA™ LTI (Invivo Biomaterial Solutions Ltd., Thornton Cleveleys, UK)	Indimatec HPP 15S/Gen2; Apmu Additive Technologies GmbH, Karlsruhe, Germany	Printing speed Annealing temperature Other parameters	1500, 2000 mm/min 200, 300 °C Nozzle diameter = 0.4 mm; nozzle temperature = 390–410 °C; bed temperature = 100 °C; layer thickness = 0.1 mm; infill pattern—rectangle; infill ratio = 100%	Compression, compression-shear, and torsion tests
Li et al. [26]	2019	PEEK (grade: ZAPEEK 550 G)	FUNMAT HT FDM 3D printer (INRAMSYS, Shanghai, China)	Parameters	Nozzle diameter = 0.4 mm Nozzle temperature = 400 °C Ambient temperature = 90 °C Platform temperature = 160 °C Nozzle moving speed = 15 mm/s Layer thickness = 0.1 mm Raster angle = +45°/−45° Air gap = 0.18 mm	Flexural and bending test, DSC, and X-ray $\mu$ -CT

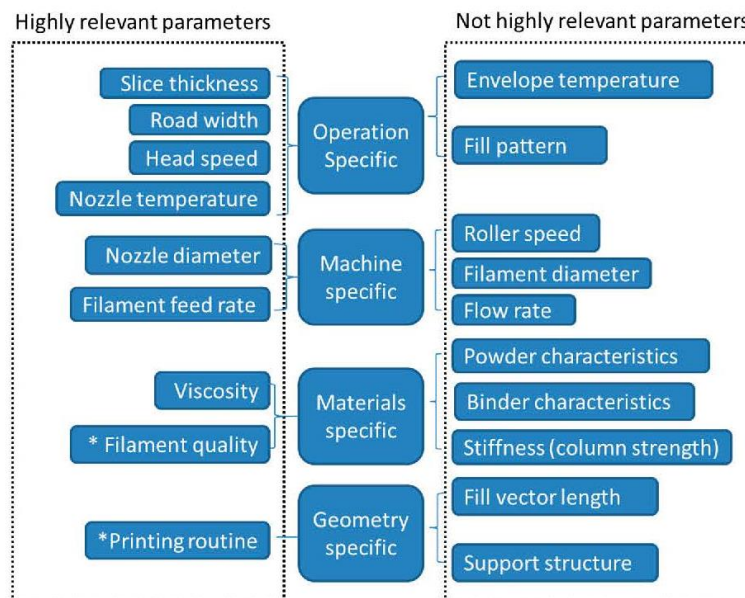
Table 2. Influence of PEEK processing parameters on mechanical properties.

Author	Year	Most Significant Parameters	Tensile Test			Bending Test			Compression Test		
			Tensile Strength (Mpa)	Tensile Modulus (Gpa)	Tensile Strength (Mpa)	Bending Strength (Mpa)	Bending Modulus (Gpa)	Compressive Strength (Mpa)	Compressive Modulus (Gpa)		
Wu et al. [16]	2015	Layer thickness = 300 $\mu$ m, raster angle = 0/90°	56.60		56.10					60.90	
Vaezi et al. [17]	2015	100% infill rate PEEK /	75.06		132.37		2.43			102.38	
Rahman et al. [18]	2016	Infill = 100%; layer height = 0.25 mm; extruder temperature = 340 °C; platform temperature = 230 °C; printing speed = 50 mm/s; raster angle = 0°	73.00	2.6–2.8	111.70	1.8–1.9				80.90	2.00
Yang et al. [13]	2017	Nozzle temperature = 420 °C Cooling method—annealing Ambient temperature = 150 °C	59.00 81.50 85.00	3.10 3.90 3.90							
Berretta et al. [19]	2017	PEEK 450 G (380 °C) 1% CNT PEEK 450 G (365 °C) 5% CNT PEEK 450 G (350 °C)	90.00 90.00 94.00								
Cicala et al. [21]	2018	/	69.04 $\pm$ 7.01	3.53 $\pm$ 0.01							
Deng et al. [20]	2018	Printing speed = 60 mm/s; layer thickness = 0.25 mm; printing temperature = 370 °C; filling rate = 60%	40 $\pm$ 4.4	0.50							
Han et al. [23]	2019	PEEK CFR-PEEK	95.21 $\pm$ 1.86 101.41 $\pm$ 4.23	3.79 $\pm$ 0.27 7.37 $\pm$ 1.22	140.83 $\pm$ 1.97 159.25 $\pm$ 13.54	3.56 $\pm$ 0.13 5.41 $\pm$ 0.51			138.63 $\pm$ 2.69 137.11 $\pm$ 3.43	2.79 $\pm$ 0.11 3.51 $\pm$ 2.12	
Li et al. [26]	2019	PEEK CF-PEEK			146 $\pm$ 3.3 146 $\pm$ 4.2	3.44 $\pm$ 0.05 3.74 $\pm$ 0.09					
Hu et al. [24]	2019	PEEK	74.70	1.15	120.20	1.15					
Reference	/	VICTREX® PEEK 450 G molded PEEK	98.00	4.00	165.00	3.80			125.00	3.80	

Methods for the characterization of printed PEEK samples are mainly scanning electron microscope (SEM) [15,22,23], 3D scanner [15], differential scanning calorimetry (DSC) [13], and water contact angle measurements [23]. These methods mainly assess the dimensional accuracy, surface roughness, microstructure of interface, and crystalline ratio of printed PEEK objects.

The reviewed articles conducting mechanical tests of 3D printed PEEK show that temperature, raster angle, layer thickness, filling ratio, and printing speed are the main factors influencing the mechanical properties of printed PEEK. The maximal tensile, bending, and compression strength of 3D printed pure PEEK specimens are similar or even better than the reference as seen in Table 2. Carbon-fiber-reinforced PEEK performs as a substitute for traditionally processed PEEK [19,23,26].

According to the literature, understanding the properties of PEEK and the settings of the printer are most important to achieve satisfying results. To expand PEEK application in dentistry, more efforts in exploring parameters need to be made. Based on the theory of Agarwala et al. [27], as well as our own researches, the most concerned parameters for printing small PEEK parts are listed in Figure 2. In the special case of PEEK printing with FDM, the not highly related parameters are either not involved, such as power characteristics and binder characteristics, or of secondary priority for small parts, such as fill pattern and support structure.



\* are the parameters that came up with according to our own research; the rest are mentioned in [27].

**Figure 2.** Schematic diagram of parameters that have effects on small PEEK parts made from FDM [27].

#### 4. Discussion

In this part, we talk about the parameter matters for small printed PEEK objects as summarized in the schematic diagram.

##### 4.1. Review of Literature and Printing Parameter Settings

###### 4.1.1. Viscosity and Specific Thermal Properties of PEEK

Some physical characteristics of PEEK related to 3D printing are shown in Table 3. PEEK, as a semi-crystalline polymer, has exceptional properties than other thermoplastic materials regarding its high  $T_m$  and  $T_g$ . PEEK has crystalline and amorphous domains: the macromolecular chains in the

crystalline region align in better order and own stronger intermolecular forces, causing greater strength and rigidity. The macromolecular chains in the amorphous region prefer to intertwine loosely and are easy to be scattered and stretched, showing good extensibility [28]. Generally, thermoplastics need to be heated at least beyond the  $T_g$  to be processed. Since reaching glass transition temperature is not enough to break the crystal lattice, the FDM processing temperature used for PEEK printing is far above  $T_g$ , when both crystalline and non-crystalline phase are flexible. The detailed temperature for printing is explained in Section 4.1.2.

**Table 3.** Some performance of unfilled PEEK important for 3D printing.

Performance		Testing Method/Standard	Value	Reference
Density	Crystalline	ASTM D792	1.32 g/cm <sup>-3</sup>	[1]
Typical crystalline ratio		N/A	35%	[13]
Melting temperature ( $T_m$ )		DSC	343 °C	[1]
Glass transition temperature ( $T_g$ )		DSC	143 °C	[1]
Coefficient of thermal expansion (CTE)	< $T_g$	ASTM D696	5.5 × 10 <sup>-5</sup> K <sup>-1</sup>	VICTREX®
	> $T_g$		14.0 × 10 <sup>-5</sup> K <sup>-1</sup>	
Heat deflection temperature (HDT)		ASTM D648	152 °C	VICTREX®

The coefficient of thermal expansion (CTE) is another factor that has an influence on PEEK printing quality. The CTE of PEEK is 5.5 × 10<sup>-5</sup> K<sup>-1</sup> below the temperature of 143 °C, and 14.0 × 10<sup>-5</sup> K<sup>-1</sup> above  $T_g$ . Assuming printing a PEEK part with a nozzle temperature of 380 °C, it is divided into two phases, above and below  $T_g$ . In the first phase when the material is extruded, it cools down rapidly from 380 °C to ambient temperature. During the first phase, the  $\Delta L/L$  is 3.3%, which is the linear shrinkage deformation rate of the sample. During the second phase from  $T_g$  to room temperature (25 °C), the length deformation variance is 0.6%. Wu et al. [15] reported that the warping deformation using FDM is minimal with a chamber temperature of 130 °C and a nozzle temperature of 350 °C. In their single factor experiment, as the chamber temperature increases from 90 °C to 130 °C, the sample deformation is reduced significantly. Hu et al. [24] reported that they decreased the warpage of PEEK parts' edge from 20.4% to 5.0% by applying higher chamber temperature, adding a heat collector module, a new heater to the nozzle, and using a PEEK substrate. Dimensional variance should be taken into consideration before printing when setting the dimension compensation parameters. This shrinkage may be tolerable when printing simple shapes, e.g., medical substitutes of mandibular or ribs, when preciseness is not an issue. Regarding small devices with an elaborate design, this imprecision is not acceptable. In conclusion, delicate control of the temperature field in the print area is an important way to reduce deformation and warpage.

Viscosity of the material should also be taken into consideration during the FDM procedure. Wang et al. [29] made a finite element analysis (FEA) of PEEK material in the flow channel of the nozzle to explore reasonable printing temperatures. According to their experiment, the heating temperature of the printing head, wire feeding speed, and diameter of the nozzle are the key parameters influencing the distribution of the temperature field, viscosity field, and pressure field. To summarize from their experiment, higher temperature and slower feeding speed guarantee a longer length of the liquid column in the nozzle (Figure 3), and therefore confirm better processing possibility of the material.

#### 4.1.2. Temperature

Nozzle temperature, plate temperature, chamber/ambient temperature, and cooling methods during PEEK printing have a pronounced influence on the crystallization process and therefore affect the properties of finished objects to a large extent [13].

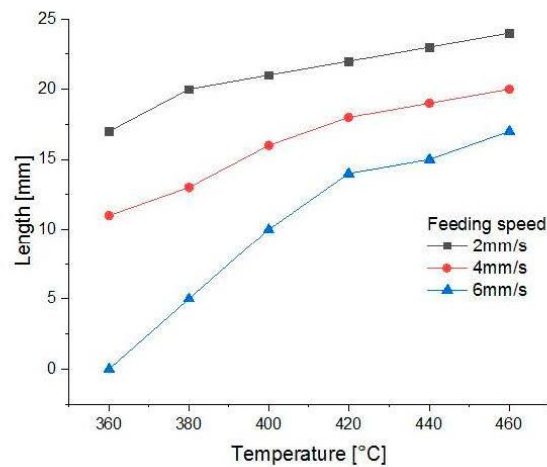


**Figure 3.** Length of the liquid column in the nozzle with diameter of 0.8 mm using the data from Wang et al. [29].

Suitable nozzle temperature can guarantee sufficient time to heat the PEEK filament. If the nozzle temperature is too low, the PEEK filament is not melted completely, which may lead to nozzle obstruction because of the high viscosity of the material. If the nozzle temperature is too high, chain cleavage might occur and possibly leading to decomposition [15]. Nozzle temperatures have been explored within a range from 340 °C to 480 °C [13,15–18,20–23]. Wu et al. [15] found when the nozzle temperature is 350 °C, the warping deformation of PEEK samples is minimal. Vaezi et al. [17] identified nozzle temperatures of 400–430 °C as an applicable range. Nozzle temperatures below 400 °C caused either nozzle clogging or delamination of the final product, and above 430 °C resulted in either considerable filament deformation or material degradation. Hu et al. [24] designed a new heater control nozzle module to improve the temperature uniformity in the printing area. They used 385 °C for nozzle temperature in the experiment and reported samples with less warpage and delamination. Wang et al. [29] came up with the conclusion that considering the printing head design and size of the heating block, the length of the nozzle is recommended to be less than 15 mm, and the applicable temperature for PEEK printing should be in the range between 380 °C to 440 °C. Yang et al. [13] applied 360 °C–480 °C in their experiments and used a gradient of 20 °C. Nozzle temperature was found to be a complicated factor for the PEEK's crystallinity and mechanical properties. When the nozzle temperature increased from 360 °C to 380 °C, the crystallinity first was reduced from 19% to 16%, which can be explained as an incomplete melting of crystalline regions inside the nozzle with a lower and non-uniform temperature. Then, the crystallinity turned into a moderate growth until a relatively stable value (21%) as the nozzle temperature increased up to 480 °C. Higher crystallinity samples performed better mechanical strength, which is shown in Table 2. To sum up, the quality and characteristics of filaments from different companies may account for the difference between these results. The filaments vary from each other so the most suitable printing temperature needs to be explored before the experiment. Taking the two kinds of filaments we applied in our research as examples, filaments made by Evonik can be printed continuously when nozzle temperature is between 420 and 440 °C, while the suitable temperature range for the Apium filaments is 380–400 °C. The reason lies in the purity of the filament. Possible contamination is the filament could be wax, which is brought in during filament manufacture.

Platform temperature, chamber/ambient temperatures, and cooling methods have a direct or indirect impact on the cooling speed of the samples and sequentially affect the crystallinity of the products. Most of the authors used air cooling as cooling methods, while others also explored different cooling methods such as furnace cooling, quenching, annealing, and tempering. Wu et al. [15] came



to the conclusion that 130 °C is the most suitable chamber temperature for PEEK printing, while Hu et al. [24] applied 135 °C as plate temperature. Vaezi et al. [17] identified a plate temperature of 130 °C and an ambient temperature of 80 °C as applicable conditions for an extrusion rate of 2.2 mg/s. Han et al. [23] kept the printed PEEK samples in a furnace for 2 h at 300 °C, and let them cool down at room temperature afterward. When the temperature rises above  $T_g$ , there will be a thermodynamic tendency for the polymer to continue to form crystals or to recrystallize [1]. This procedure increased the time for crystalline and may account for the better mechanical performance of the samples. Yang et al. [13] obtained similar results and concluded in their experiment that the higher ambient temperatures would provide more energy and time to improve the crystallinity of PEEK. Furnace and annealing cooling permit samples to stay in temperatures beyond  $T_g$ , causing an isothermal crystallization process, in which the amorphous polymer chains have sufficient energy to transform and crystallize to a degree of around 31%, but still less than the typical crystallinity (35%). In contrast, rapid cooling of PEEK samples, such as quenching and tempering methods, can cause warp distortion, caused by uneven crystallization, because the internal stress leads to significant deformation [13]. Basgul et al. [25] conducted experiments on annealing to seek a possible post-processing method for printed PEEK parts as lumbar spinal cages. They observed that the annealing effect increased the cages' mechanical properties (14% increases in compression strength) printed with slower speed, indicating annealing might enhance the interlayer adhesion under certain printing conditions. They also concluded that annealing can change the structure of the pores but is not able to decrease the undesired porosity formed during the 3D printing process.

#### 4.1.3. Layer Thickness and Printing Speed

The layer thickness plays key roles in determining the dimensional accuracy and the surface roughness of printed parts [30]. The surfaces of printed objects made by AM exhibit ridges caused inherently by the deposition process. Theoretically, if the layer height is small enough, the surface of the specimens will be smooth. However, the typical minimum feature size obtained with an extrusion AM process is in the order of 100  $\mu\text{m}$  [12]. The authors in the reviewed literature applied different layer heights, which are between 0.1 mm and 0.4 mm. The work of Wu et al. [16] showed that optimal mechanical properties were found in samples with a layer thickness of 0.3 mm. Deng et al. [20] demonstrated that an optimal tensile strength and elongation rate can be achieved when the parameter of layer thickness is 0.25 mm, while the optimal elastic modulus is achieved when the layer thickness is 0.2 mm.

Printing speed is another important factor in 3D printing. If the extrusion speed does not match with the printing speed, there will be extra material sticking to the nozzle causing unstable dimensions of the printed specimens. Geng et al. [22] investigated the effects of the extrusion and printing speed on the microstructure and dimensions of an extruded PEEK filament. They performed the experiments with nozzle diameters of 0.4, 0.5, and 0.6 mm and printing speeds from 0.1 to 120 mm/min. They concluded that during the FDM of PEEK, the melt pressure directly affects the surface morphology and extrusion diameter of the filament, and higher melt pressure is beneficial for the reduction of surface defects on the extruded filament. Rahman et al. [18] took a printing speed of 50 mm/s in their experiments while Han et al. [23] applied a printing speed of 40 mm/s in theirs. Deng et al. [20] achieved optimal tensile properties for PEEK specimens when the printing speed was 60 mm/s. According to the results above, we can assume that a reasonable speed value for the printing of PEEK with a 0.4 mm diameter nozzle should lie in the range of 40–80 mm/s.

The fluctuating extrusion force is the main constraint on the stability of the extrusion process [22]. As shown in Figure 4, the effect of viscosity of the material on extrusion, retraction distance (which means the distance of retraction after printing each layer, usually between 1 and 5 mm), and extrusion multiplier should also be taken into consideration. In short, if the volume of the material extruded from the nozzle is not appropriately synchronized with the volume of material needed for deposition, then it would create either an overflow of polymers or deflection of structure flaw of finished parts.

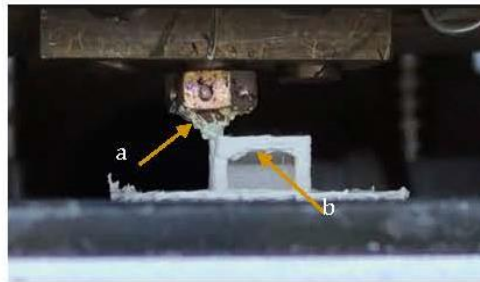


**Figure 4.** A shot of the 3D printer in the processing of DC4430 PEEK. (a) The residual material sticking to the nozzle. (b) The structure defect of sample.

#### 4.1.4. Nozzle Diameter and Nozzle Material

To improve the accuracy of the finished parts, reducing the nozzle diameter seems to be a possible way. Simply decreasing the nozzle diameter will more easily cause blocking of the nozzle and cannot solve the problem of low resolution completely. In the reported literature, nozzles with diameters between 0.2 mm and 0.8 mm are generally applied [18,20,22,23,29]. Wang et al. [29] observed that from the enlarged pressure field of the flow channel, extrusion pressure at the outlet of the nozzle is 10 percent of its original value, as it drops from  $5.5 \times 10^4$  Pa to  $0.45 \times 10^4$  Pa, and the diameter of nozzle varies from 0.4 mm to 0.8 mm. A larger diameter nozzle can therefore effectively reduce the wire feeding pressure of the extruder and enlarge the printing layer thickness, which may be favorable for the life of the extruder motor but disadvantageous for the surface quality of the finished part.

The key for accurate manipulation is controlling precisely the outflow of the material, which has to be explored as each individual printing depicts the design of finished objects. However, the principal resolution of the printer software is limited; there is no value to improve the file resolution beyond the recognition of achievable stepper motors in extruded AM systems [30].

Commercially, extrusion printing heads for PEEK printing are commonly made of brass or stainless steel [17]. They are widely used because of their excellent heat-conducting property and resistance to high temperatures. However, metals have a trend of thermal dissipation, which results in the inaccuracy of live temperature during the printing process. Therefore, ceramics might be a possible alternative material as nozzle heads. They have a lower coefficient of thermal expansion and maintain the heat within a certain zone better.

#### 4.1.5. Starting Point and Software

The printing routine/toolpath is one of the key design variables in the production of parts via extrusion-based additive processes [30]. However, in all the reviewed literature concerning PEEK printing, this parameter was not been mentioned as one of the key parameters affecting the quality of samples.

To establish a uniform surface, the contour is typically printed around the perimeter of a part. In our experiment, we used two software; one was the printer implemented software and the other was Simplify 3D. When printing a cylinder, samples coded by Simplify 3D software are constructed with reciprocating lines, which means the nozzle is moving clockwise and anticlockwise for one round, and then the printing platform moves up and down to adjust itself for the next layer. On the contrary, software installed in the machine has a different routine. The nozzle moved in one direction all the time, with the platform adjusting its position in the Z-axis almost in the same position. When printing samples with relatively great dimensions—for example, hollow cylinders with an outer radius of 5 mm and a wall thickness of 0.5 mm—there was no significant difference between samples. However, when we reduced the diameter gradually, and approached a radius of 3 mm, the routine used reciprocating lines around one layer had a “V” split line along the starting point (Figure 5). We

observed during the printing procedure that the semi-liquid extruded PEEK tended to retract for the starting point because of inner tension; suddenly, a veer of the nozzle dragged the extruded material away. This result may indicate that the back and forth routine has higher requirements for calibration than the mono-directional routine. What is more, we deduce that different slicers may account for this phenomenon, leading to some printing defects in the printing process.

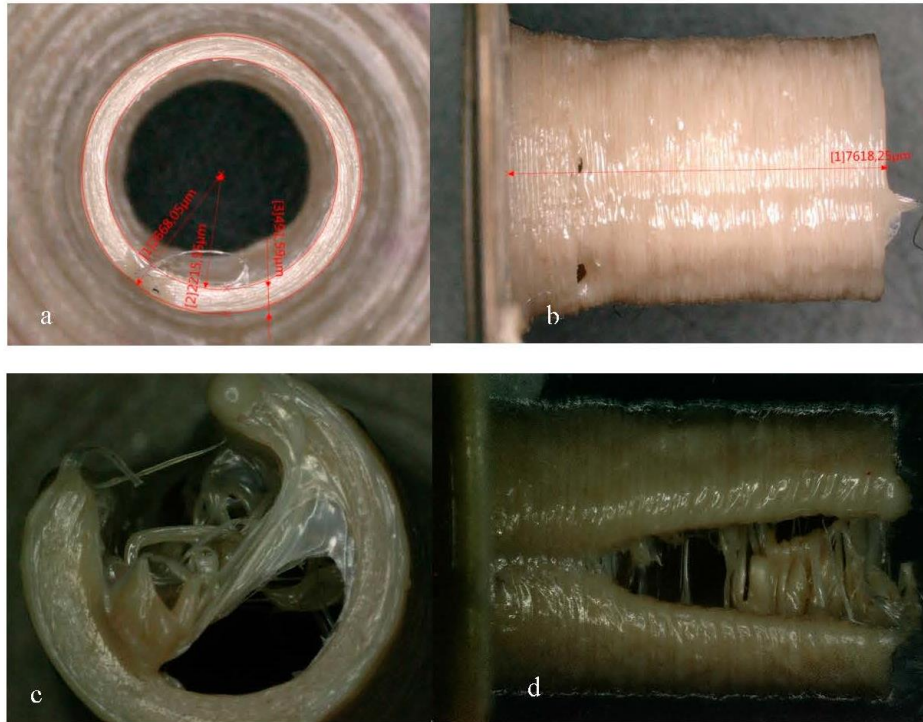


**Figure 5.** Barrels printed with radius of 3 mm and wall thickness of 0.5 mm by Apium HPP155 with two software. (a,b) Samples printed by software installed in the printer, and (c,d) are printed by Simplify 3D, respectively.

Another interesting phenomenon found in our experiment is that the bottom layers in general have a greater diameter than the upper rim or disk, respectively, resembling an “elephant foot” (Figure 5). This is a popular problem that happened in the FDM strategy. If the bottom layer of the model does not have enough time to cool down during the printing process, then the bottom layer is pressed by the weight of the upper part of the model, which will cause the bottom layer to protrude outward. This situation is more likely to occur especially when the bed temperature setting of the 3D printer is too high. Possible solutions lie in the better calibration of the plate, the fitter distance between the nozzle and plate, as well as a nice setting of plate temperature and cooling fan.

## 5. Own Experiments

A dental implant made of PEEK has better advantages than titanium ones, as it can reduce the risk of allergy and its similar elastic modulus with bone, therefore it can decrease the stress-shielding phenomenon in the site of surgery. Based on the experiences from the literature survey, it was tried to print a dental implant with an inner and outer structure using a commercially available 3D printer for PEEK from Apium (Karlsruhe, Germany) as well as a printer from Orion (Berlin, Germany).

### 5.1. Implant Printed with an Apium HPP155 Printer

We printed a magnified dental implant that is almost three times in dimension of a real one, applying the optimal parameters we got from others' experience as well as our own trials, to explore the possibility of producing a dental implant with the FDM strategy. As we can see from the image (Figure 6), both the inner and outer screw depth of the implant is not acceptable and the porosity of the sample is evident. The detailed parameters for printing are shown in Table 4. The elastic modulus of the sample is 0.89 GPa, which is 25% of Young's modulus of the molded PEEK (3.6 GPa). Implants with smaller dimensions were also tried but all of them failed. Since there is no matching substitute nozzle with a smaller nozzle diameter for this printer, we tried to print the implant with another printer from Orion, which was more flexible in nozzle and heater settings.

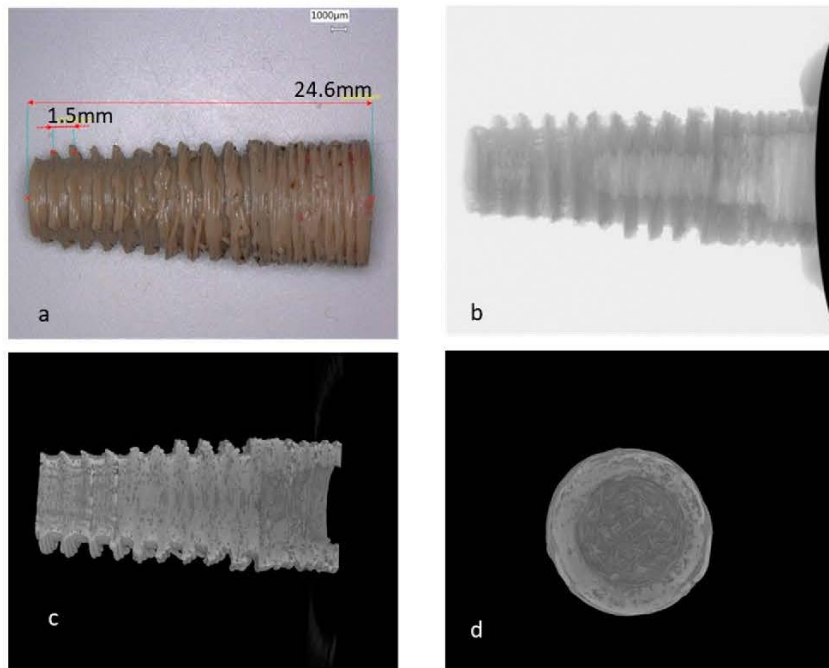


**Figure 6.** CT of a magnified dental implant produced with Apium HPP155 ((a) is the printed implant, (b–d) are micro CTs of the sample).

**Table 4.** The parameters used for dental implant printed with Apium HPP155 printer.

Parameters	Value
Filament diameter	1.75 mm
Nozzle diameter	0.4 mm
Nozzle temperature	395 °C
Printing speed	13 mm/s
Layer thickness	0.1 mm
Slicer	Machine-installed slicer

### 5.2. Implants Printed with Orion Printer

We printed the same dental implant STL file with the second-generation printer of Orion and got better results, as shown in Figure 7. The smallest successfully printed implant is with a width of 3.6 mm and a length of 9.4 mm, which is a little crooked. We got the best specimens with the 0.15 mm nozzle when printing the  $\times 1.2$  scale implant, which is acceptable in both the reproducibility and surface quality. The parameters for printing are shown in Table 5. The elastic modulus of the implants is

$2.3 \pm 0.28$  GPa. This value is within the range of the elastic modulus of cancellous bone suitable for implant surgery, which is between 1.5 GPa and 7.9 GPa [31]. However, smaller nozzles will inevitably lead to longer printing time and are easier to be clogged. This may be ignorable at the research phase, but will increase the cost of manufacturing in mass.

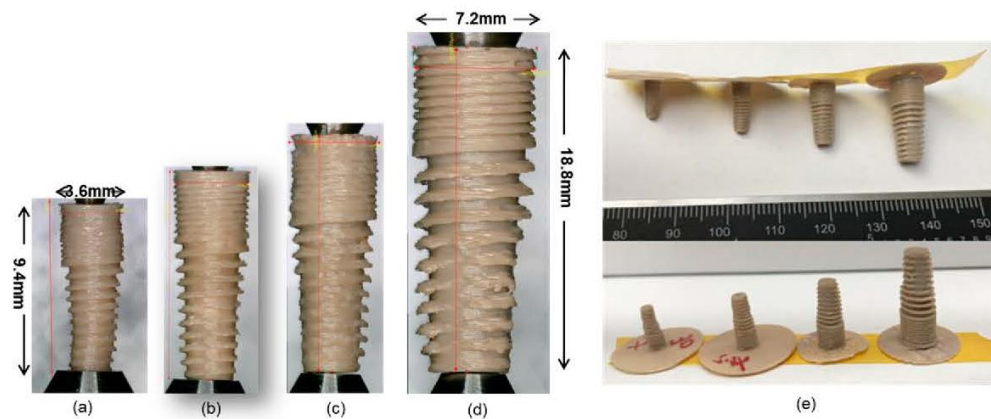


**Figure 7.** Dental implants printed with Orion Generation 2 ((b–d) are  $\times 1.2$ ,  $\times 1.5$ , and  $\times 2$  scale of a separately; (a,b) are printed with a 0.15 mm nozzle at the temperature of 405 °C; (c) is printed with a 0.2 mm nozzle at a temperature of 390 °C; (d) is printed with a 0.4 mm nozzle at a temperature of 390 °C, (e) is the group photo of the above samples).

**Table 5.** The parameters used for a  $\times 1.2$  scale dental implant printed with the second-generation printer of Orion.

Parameters	Value
Filament diameter	1.75 mm
Nozzle diameter	0.15 mm
Nozzle temperature	405 °C
Chamber temperature	250 °C
Plate temperature	250 °C
Layer heater	200 °C
Printing speed	400 mm/min
Layer thickness	0.05 mm
Slicer	Simplify 3D
Printing time	49 m 12 s

## 6. Conclusions

The patient-orientated therapy model is now drawing efforts to precisely manufactured dental devices and attachments in the dentistry field. Three-dimensional printing is with no doubt an alternative way to accomplish this goal. Considering the great mechanical properties and reliable biocompatibility of PEEK, it has great potential to be used as a substitute for medical devices, and 3D printing strategy offers a promising way of process production and manufacture.

Knowing that for these tests, the last developed machine was not used, we could demonstrate the limits, which drove us to the conclusion that it is necessary to adjust the following parameters. For the most widely applied brass nozzle with a diameter of 0.4 mm, its temperature should be maintained within 380 °C–420 °C, the purity of the filament should be taken into consideration, and pre-tests are recommended before the experiment. A constancy of nozzle temperature is better controlled in a range of  $\pm 1$  degree. Printing speed and retraction speed should be considerably tested considering PEEK types and manufacturers, with the purpose to make the extruded material match with that desired for

construction. Further improvement of samples with improved mechanical strength might count on the better solution of 3D printer technology and better manipulation of PEEK.

Until now, the printing of reproducible tiny-sized PEEK parts with high accuracy has proved to be possible in our experiments, which is achieved through optimization of the FDM printing parameters. There is still a long way to go to accomplish the transition from the research phase to 3D printed PEEK manufacturing, and finally to reach the goal of integrating the treatment within clinics. However, this trial might lay a basis for the patient-specialized treatment in the field of dental implantology. Considering the complexity of chewing forces, systematical mechanical tests are needed, and simulation based on finite element analysis is necessary for further research.

**Author Contributions:** Conceptualization, investigation, and writing—original draft preparation, Y.W.; conceptualization, funding acquisition, project administration, resources, writing—review and editing, and supervision, W.-D.M.; investigation and resources, A.R.; conceptualization, funding acquisition, project administration, writing—review and editing, and supervision, A.S. All authors have read and agreed to the published version of the manuscript.

**Funding:** This research was funded by the China Scholarship Council (CSC), grant number 201706240007.

**Acknowledgments:** Thank you for the generous donation of Apium company for the 3D PEEK printer HPP155 and also for the supports of Orion company. Thanks to Dr. Matthias Gabriel for reviewing and editing the manuscript.

**Conflicts of Interest:** We declare that we do not have any commercial or associative interest that represents a conflict of interest in connection with the work submitted.

## References

1. Kurtz, S.M. *An Overview of PEEK Biomaterials*; Elsevier Inc.: Amsterdam, The Netherlands, 2012.
2. Mark, H.F. *Encyclopedia of Polymer Science and Technology*; John Wiley & Sons: Hoboken, NJ, USA, 2001.
3. Kurtz, S.M.; Devine, J.N. PEEK biomaterials in trauma, orthopedic, and spinal implants. *Biomaterials* **2007**, *28*, 4845–4869. [[CrossRef](#)] [[PubMed](#)]
4. Lu, S.X.; Cebe, P.; Capel, M. Thermal stability and thermal expansion studies of PEEK and related polyimides. *Polymer* **1996**, *37*, 2999–3009. [[CrossRef](#)]
5. Green, S.; Schlegel, J. A polyaryletherketone biomaterial for use in medical implant applications. In Proceedings of the Polymers for the Medical Industry, Brussels, Belgium, 14–15 May 2001.
6. Liao, K. Performance characterization and modeling of a composite hip prosthesis. *Exp. Tech.* **1994**, *18*, 33–38. [[CrossRef](#)]
7. Maharaj, G.R.; Jamison, R.D. *Intraoperative Impact: Characterization and Laboratory Simulation on Composite Hip Prostheses*; Jamison, R.D., Gilbertson, L.N., Eds.; ASTM International: West Conshohocken, PA, USA, 1993.
8. Kelsey, D.J.; Springer, G.S.; Goodman, S.B. Composite Implant for Bone Replacement. *J. Compos. Mater.* **1997**, *31*, 1593–1632. [[CrossRef](#)]
9. Kurtz, S.M. *Synthesis and Processing of PEEK for Surgical Implants*; Elsevier Inc.: Amsterdam, The Netherlands, 2012.
10. Schmidt, M.; Pohle, D.; Rechtenwald, T. Selective Laser Sintering of PEEK. *CIRP Ann.* **2007**, *56*, 205–208. [[CrossRef](#)]
11. Lee, C.-U. Room Temperature Extrusion 3D Printing of Polyether Ether Ketone Using a Stimuli-Responsive Binder. *Bull. Am.* **2019**, *28*, 430–438. [[CrossRef](#)]
12. Turner, B.N.; Strong, R.; Gold, S.A. A review of melt extrusion additive manufacturing processes: I. Process design and modeling. *Rapid Prototyp. J.* **2014**, *20*, 192–204. [[CrossRef](#)]
13. Yang, C.; Tian, X.; Li, D.; Cao, Y.; Zhao, F.; Shi, C. Influence of thermal processing conditions in 3D printing on the crystallinity and mechanical properties of PEEK material. *J. Mater. Process. Technol.* **2017**, *248*, 1–7. [[CrossRef](#)]
14. Dawood, A.; Marti, B.M.; Sauret-Jackson, V.; Darwood, A. 3D printing in dentistry. *Br. Dent. J.* **2015**, *219*, 521–529. [[CrossRef](#)]
15. Wu, W.Z.; Geng, P.; Zhao, J.; Zhang, Y.; Rosen, D.W.; Zhang, H.B. Manufacture and thermal deformation analysis of semicrystalline polymer polyether ether ketone by 3D printing. *Mater. Res. Innov.* **2014**, *18*, S5-12–S5-16. [[CrossRef](#)]

16. Wu, W.; Geng, P.; Li, G.; Zhao, D.; Zhang, H.; Zhao, J. Influence of layer thickness and raster angle on the mechanical properties of 3D-printed PEEK and a comparative mechanical study between PEEK and ABS. *Materials* **2015**, *8*, 5834–5846. [[CrossRef](#)] [[PubMed](#)]
17. Vaezi, M.; Yang, S. Extrusion-based additive manufacturing of PEEK for biomedical applications. *Virtual Phys. Prototyp.* **2015**, *10*, 123–135. [[CrossRef](#)]
18. Rahman, K.M.; Letcher, T.; Reese, R. *Mechanical Properties of Additively Manufactured PEEK Components Using Fused Filament Fabrication*; V02AT02A009; American Society of Mechanical Engineers: New York, NY, USA, 2016.
19. Berretta, S.; Davies, R.; Shyng, Y.T.; Wang, Y.; Ghita, O. Fused Deposition Modelling of high temperature polymers: Exploring CNT PEEK composites. *Polym. Test.* **2017**, *63*, 251–262. [[CrossRef](#)]
20. Deng, X.; Zeng, Z.; Peng, B.; Yan, S.; Ke, W. Mechanical properties optimization of poly-ether-ether-ketone via fused deposition modeling. *Materials* **2018**, *11*, 216. [[CrossRef](#)] [[PubMed](#)]
21. Cicala, G.; Latteri, A.; Recca, G.; Lo Russo, A.; Farè, S.; Del Curto, B. Engineering Thermoplastics for Additive Manufacturing: A Critical Perspective with Experimental Evidence to Support Functional Applications. *J. Appl. Biomater. Funct. Mater.* **2018**, *15*, 10–18. [[CrossRef](#)]
22. Geng, P.; Zhao, J.; Wu, W.; Ye, W.; Wang, Y.; Wang, S.; Zhang, S. Effects of extrusion speed and printing speed on the 3D printing stability of extruded PEEK filament. *J. Manuf. Process.* **2019**, *37*, 266–273. [[CrossRef](#)]
23. Han, X.; Yang, D.; Yang, C.; Spintzyk, S.; Scheideler, L.; Li, P.; Li, D.; Geis-Gerstorf, J.; Rupp, F. Carbon Fiber Reinforced PEEK Composites Based on 3D-Printing Technology for Orthopedic and Dental Applications. *J. Clin. Med.* **2019**, *8*, 240. [[CrossRef](#)]
24. Hu, B.; Duan, X.; Xing, Z.; Xu, Z.; Du, C.; Zhou, H.; Chen, R.; Shan, B. Improved design of fused deposition modeling equipment for 3D printing of high-performance PEEK parts. *Mech. Mater.* **2019**, *137*, 103139. [[CrossRef](#)]
25. Basgul, C.; Yu, T.; MacDonald, D.W.; Siskey, R.; Marcolongo, M.; Kurtz, S.M. Does annealing improve the interlayer adhesion and structural integrity of FFF 3D printed PEEK lumbar spinal cages? *J. Mech. Behav. Biomed. Mater.* **2020**, *102*, 103455. [[CrossRef](#)]
26. Li, Q.; Zhao, W.; Li, Y.; Yang, W.; Wang, G. Flexural properties and fracture behavior of CF/PEEK in orthogonal building orientation by FDM: Microstructure and mechanism. *Polymers* **2019**, *11*, 656. [[CrossRef](#)]
27. Agarwala, M.K.; Jamalabad, V.R.; Langrana, N.A.; Safari, A.; Whalen, P.J.; Danforth, S.C.; Agarwala, M.K.; Jamalabad, V.R.; Langrana, N.A.; Safari, A.; et al. Structural quality of parts processed by fused deposition. *Rapid Prototyp. J.* **1996**, *2*, 4–19. [[CrossRef](#)]
28. Mark, J.E. *Physical Properties of Polymers Handbook*; Springer: New York, NY, USA, 2007.
29. Wang, P.; Zou, B.; Xiao, H.; Ding, S.; Huang, C. Effects of printing parameters of fused deposition modeling on mechanical properties, surface quality, and microstructure of PEEK. *J. Mater. Process. Technol.* **2019**, *271*, 62–74. [[CrossRef](#)]
30. Turner, B.N.; Gold, S.A. A review of melt extrusion additive manufacturing processes: II. Materials, dimensional accuracy, and surface roughness. *Rapid Prototyp. J.* **2015**, *21*, 250–261. [[CrossRef](#)]
31. Cook, S.D.; Klawitter, J.J.; Weinstein, A.M. The influence of implant elastic modulus on the stress distribution around LTI carbon and aluminum oxide dental implants. *J. Biomed. Mater. Res.* **1981**, *15*, 879–887. [[CrossRef](#)]



© 2020 by the authors. Licensee MDPI, Basel, Switzerland. This article is an open access article distributed under the terms and conditions of the Creative Commons Attribution (CC BY) license (<http://creativecommons.org/licenses/by/4.0/>).

## **Curriculum Vitae**

My curriculum vitae does not appear in the electronic version of my paper for reasons of data protection.



## Publication List

1. **Wang Y**, Müller W, Rumjahn A, Schwitalla A. Parameters Influencing the Outcome of Additive Manufacturing of Tiny Medical Devices Based on PEEK [J]. Materials (Basel) 2020, 13(2), 466.

→Journal impact factor: 2.972

2. **Wang Y**, Müller W, Rumjahn A, Schmidt F, Schwitalla A. Mechanical properties of fused filament fabricated PEEK for biomedical applications depending on 3D printing parameters [J]. Journal of the mechanical behavior of biomedical materials 2020 (115), 104250.

→Journal impact factor: 3.239

3. **Wang Y**, Rumjahn A, Müller W, Schwitalla A. Tiny dental devices printed with PEEK [C]. Transactions on Additive Manufacturing Meets Medicine, Vol 1 No S1 (2019).

This journal does not have an ISI Web of Knowledge listed Impact Factor.

4. **Wang Y**, Wang M, Liu W, Wang H. A Review of Tooth Discoloration Induced by Root Canal Therapy Materials and Medicaments [J]. Chinese Journal of Conservative Dentistry 2017, 27 (5).

This journal does not have an ISI Web of Knowledge listed Impact Factor.

5. Yu K, Liu W, Chen H, Fu T, **Wang Y**, Wang H, Tan Z. Experimental Study of Autogenously Bone Ring Graft with Simultaneous Implant Placement in Dogs [J]. Journal of Oral Science Research 2016 Apr. 32 (4)

This journal does not have an ISI Web of Knowledge listed Impact Factor.

6. Li L, Zhang B, **Wang Y**, Zhang S, Li Z, Yang Z. Knowledge of physical education teachers about emergency management of dental trauma in Chengdu [J]. Journal of Practical Stomatology 2013 Jul, 29(4).

This journal does not have an ISI Web of Knowledge listed Impact Factor.

## **Acknowledgment**

I would like to acknowledge my doctoral supervisor Prof. Dr. Wolf-Dieter Müller for inspiring my interest in the development of research and innovative technologies as well as encouraging me all the time when I was frustrated. I would also like to thank Prof. Müller and Dr. Andreas Schwitalla for the supports during the trials and for cooperation in the collection, evaluation of data and the constitution of the manuscript.

I would like to thank the China Scholarship Council (CSC) funding for covering my living expense in Germany so that I could focus on my research.

Many thanks to Adam Rumjahn, Dr. Xiangmeng Meng, Dr. Bin Wang, Dr. Jinchun Chi, Wei Li and others working in the industry field for helping me complete the basic knowledge of engineering and material so that I can accomplish my research.

Thanks to my colleagues Franziska Schmidt, Matthias Gabriel, Tycho Zimmermann, Mona S ütel, Nesreen Mohammed, Christiana Schöpfer and so on for the help in work as well as in life.

At last, I am extremely grateful to my friend Jiani Wang, Nesreen Mohammed, my boyfriend Zhongyu Wang and my parents, for your support, understanding, and accompany during these years.